

# Tetranuclear Phosphide- and Phosphinidene-Bridged Derivatives of the Diphosphenyl Complex $[\text{Mo}_2\text{Cp}_2(\mu\text{-PCy}_2)(\mu\text{-}\kappa^2\text{:}\kappa^2\text{-P}_2\text{Me})(\text{CO})_2]$

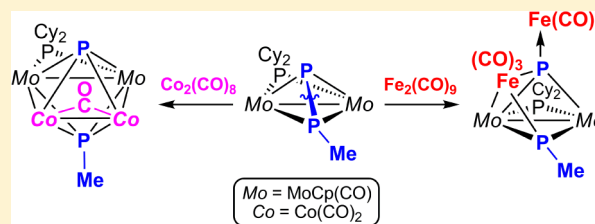
M. Angeles Alvarez,<sup>†</sup> M. Esther García,<sup>†</sup> Raquel Lozano,<sup>†</sup> Alberto Ramos,<sup>\*,‡</sup> and Miguel A. Ruiz<sup>\*,†</sup>

<sup>†</sup>Departamento de Química Orgánica e Inorgánica/IUQOEM, Universidad de Oviedo, E-33071 Oviedo, Spain

<sup>‡</sup>Instituto Nacional del Carbón, CSIC, Francisco Pintado Fe 26, E-33011 Oviedo, Spain

## Supporting Information

**ABSTRACT:** Reaction of the title complex with excess  $[\text{Fe}_2(\text{CO})_9]$  at room temperature gave the tetranuclear derivative  $[\text{Fe}_2\text{Mo}_2\text{Cp}_2(\mu_4\text{-P})(\mu\text{-PCy}_2)(\mu_3\text{-PMe})(\text{CO})_9]$ , following from formal insertion of an  $\text{Fe}(\text{CO})_3$  fragment in the P–P bond of the diphosphenyl ligand with formation of a new heterometallic bond ( $\text{Mo–Fe} = 2.935(1) \text{ \AA}$ ), and coordination of an  $\text{Fe}(\text{CO})_4$  fragment through the lone electron pair of the resulting phosphide ligand ( $\text{P–Fe} = 2.359(2) \text{ \AA}$ ). Reactions of the title complex with excess of the tetrahydrofuran (THF) adducts  $[\text{ML}_n(\text{THF})]$  ( $\text{ML}_n = \text{MnCp}'(\text{CO})_2, \text{W}(\text{CO})_5$ ) led instead to tetranuclear diphosphenyl-bridged complexes  $[\text{M}_2\text{Mo}_2\text{Cp}_2(\mu\text{-PCy}_2)(\mu\text{-}\kappa^2\text{:}\kappa^1\text{:}\kappa^1\text{-P}_2\text{Me})(\text{CO})_2\text{L}_{2n}]$  displaying a Mo–Mo double bond ( $\text{Mo–Mo} = 2.760(2) \text{ \AA}$  when  $\text{M} = \text{W}$ ), along with the phosphide- and phosphinidene-bridged complex  $[\text{Mo}_2\text{W}_2\text{Cp}_2(\mu_3\text{-P})(\mu\text{-PCy}_2)(\mu_3\text{-PMe})(\text{CO})_{10}]$ , with the latter displaying a Mo–Mo triple bond ( $\text{Mo–Mo} = 2.5542(4) \text{ \AA}$ ) and a trigonal planar phosphide ligand. Reaction of the title complex with excess  $[\text{Mo}(\text{CO})_4(\text{THF})_2]$  also resulted in facile P–P bond cleavage of the diphosphenyl ligand to give  $[\text{Mo}_4\text{Cp}_2(\mu_4\text{-P})(\mu\text{-PCy}_2)(\mu_3\text{-PMe})(\text{CO})_9]$ , a cluster built on a  $\text{Mo}_3$  triangular core bridged by phosphinidene and phosphide ligands, with the latter further coordinated to an exocyclic  $\text{Mo}(\text{CO})_5$  fragment. The related  $\text{Mo}_2\text{W}_2$  complex  $[\text{Mo}_2\text{W}_2\text{Cp}_2(\mu_3\text{-P})(\mu\text{-PCy}_2)(\mu_3\text{-PMe})(\text{CO})_9]$  could be rationally synthesized upon reaction of the trinuclear cluster  $[\text{Mo}_2\text{WCp}_2(\mu_3\text{-P})(\mu\text{-PCy}_2)(\mu_3\text{-PMe})(\text{CO})_6]$  with the adduct  $[\text{W}(\text{CO})_5(\text{THF})]$ . The title complex reacted photochemically with  $[\text{M}_2(\text{CO})_{10}]$  ( $\text{M} = \text{Mn}, \text{Re}$ ) to give the 66-electron tetranuclear derivatives  $[\text{M}_2\text{Mo}_2\text{Cp}_2(\mu_4\text{-P})(\mu\text{-PCy}_2)(\mu_3\text{-PMe})(\text{CO})_9]$ , after formation of a new Mo–M bond ( $\text{Mo–Mn} = 2.9988(7) \text{ \AA}$ ,  $\text{Mo–Re} = 3.1003(4) \text{ \AA}$ ) and cleavage of the diphosphenyl P–P bond. In contrast, its room-temperature reaction with  $[\text{Co}_2(\text{CO})_8]$  gave the 64-electron square-planar cluster  $[\text{Co}_2\text{Mo}_2\text{Cp}_2(\mu_4\text{-P})(\mu\text{-PCy}_2)(\mu_4\text{-PMe})(\mu\text{-CO})(\text{CO})_6]$  resulting from formation of two new Mo–Co bonds ( $\text{Mo–Co} = 2.8812(7) \text{ \AA}$  and  $2.9067(7) \text{ \AA}$ ) and facile P–P bond cleavage in the diphosphenyl ligand.



## INTRODUCTION

In a recent paper we initiated a study aimed toward exploring the reactivity of the diphosphenyl-bridged complex  $[\text{Mo}_2\text{Cp}_2(\mu\text{-PCy}_2)(\mu\text{-}\kappa^2\text{:}\kappa^2\text{-P}_2\text{Me})(\text{CO})_2]$  (**1**) toward suitable precursors of 16- and 14-electron metal–carbonyl fragments ( $\text{ML}_n$ ) to give novel heterometallic derivatives.<sup>1</sup> We found that, under 1:1 stoichiometric conditions, the incorporation of 16-electron fragments takes place at the apical P atom of the diphosphenyl ligand to give undetectable or unstable compounds of type  $[\text{Mo}_2\text{MCp}_2(\mu\text{-PCy}_2)(\mu_3\text{-}\kappa^2\text{:}\kappa^2\text{-P}_2\text{Me})(\text{CO})_2\text{L}_n]$  (**2**) undergoing facile P–P bond cleavage in the diphosphenyl ligand, to give either phosphide- and phosphinidene-bridged derivatives  $[\text{Mo}_2\text{MCp}_2(\mu_3\text{-P})(\mu\text{-PCy}_2)(\mu_3\text{-PMe})\text{L}_{n-1}]$  (**3**), or formal loss of “PMe” to yield novel unsaturated derivatives  $[\text{Mo}_2\text{MCp}_2(\mu_3\text{-P})(\mu\text{-PCy}_2)(\text{CO})_2\text{L}_n]$  (**4**) displaying planar trigonal phosphide ligands (Scheme 1).

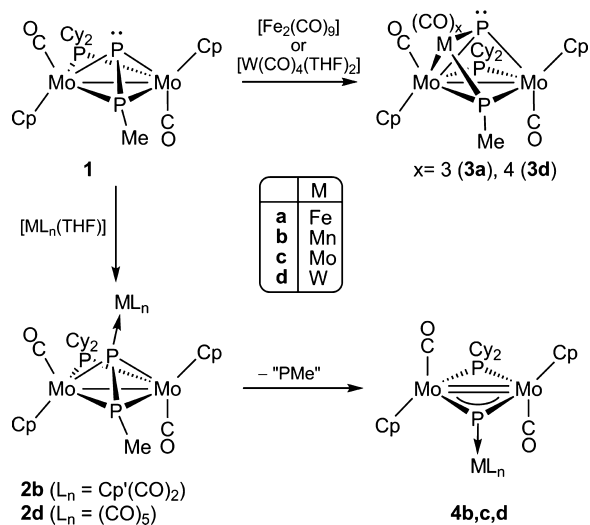
The above reactions are of interest for several reasons. In the first place, we note that the chemistry of diphosphenyl-bridged complexes is itself largely unexplored to date, particularly concerning processes that might involve the cleavage of the diphosphenyl P–P bond. Precedents for this sort of process are

limited to the reaction of the  $\mu_3$ -diphosphenyl complex  $[\text{Fe}_3\text{Cp}^*(\mu_3\text{-}\kappa^2\text{:}\kappa^2\text{-P}_2\text{tBu})(\text{CO})_8]$  with  $[\text{Fe}_2(\text{CO})_9]$  to give  $[\text{Fe}_3\text{Cp}^*\{\mu_3\text{-}\kappa^2\text{:}\kappa^2\text{-P}_2\text{PC}(\text{O})\text{P}^t\text{Bu}\}(\text{CO})_8]$ ,<sup>2</sup> and can also be found in some diphosphorus-bridged complexes such as  $[\text{Re}_2\text{Cp}^*_2(\mu\text{-}\kappa^2\text{:}\kappa^2\text{-P}_2)(\text{CO})_4]$ , a molecule reacting with  $[\text{W}(\text{CO})_5(\text{THF})]$  (THF = tetrahydrofuran) to give, *inter alia*, the phosphide complex  $[\text{W}_2\text{Re}_2\text{Cp}^*_2(\mu_3\text{-P})_2(\text{CO})_{12}]$ .<sup>3</sup> In any case, the facile cleavage of the P–P bond observed in the above reactions of **1** is remarkable if we take into account the considerable strength of this bond, as indicated by its short interatomic distance ( $2.085(1) \text{ \AA}$ ) and high P–P coupling ( $503 \text{ Hz}$ ).<sup>4</sup> On the other hand, since compound **1** is itself derived from white phosphorus via the diphosphorus-bridged anion  $[\text{Mo}_2\text{Cp}_2(\mu\text{-PCy}_2)(\mu\text{-}\kappa^2\text{:}\kappa^2\text{-P}_2)(\text{CO})_2]^-$ , the above reactions are to be considered of general interest in the context of  $\text{P}_4$  activation aimed to give different organophosphorus derivatives while avoiding synthetic routes that involve environmentally unfriendly chemicals (e.g., using chlorinated intermediates).<sup>5–8</sup>

Received: December 23, 2014

Published: February 11, 2015

Scheme 1



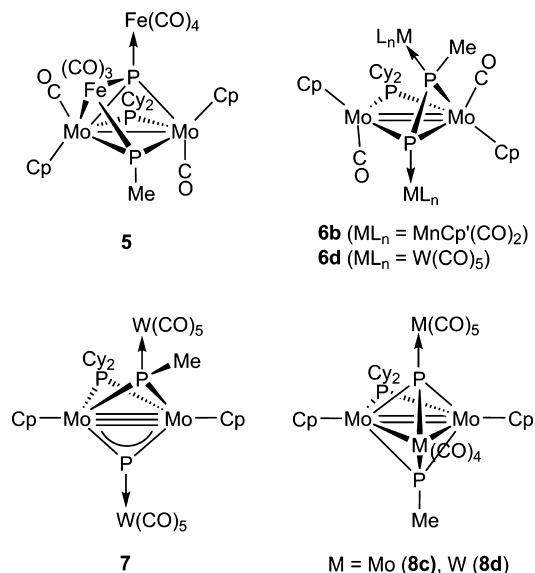
At the time we explored the reactions of **1** leading to compounds **2** to **4** we noted the need to control the stoichiometric conditions to avoid the formation of higher nuclearity species, which are instead the subject of the current paper. In particular, we here report the rational preparation of heterometallic derivatives of **1** involving the incorporation of two new metal fragments, which can be easily accomplished by reacting **1** with excess of suitable sources of the 16- or 14-electron metal-carbonyl fragments or, alternatively, upon reaction with binuclear metal carbonyls such as  $[M_2(CO)_{10}]$  ( $M = Mn, Re$ ) or  $[Co_2(CO)_8]$  under suitable conditions. As it will be shown below, a great structural variety of tetranuclear species can be formed in this way, these including 66-electron (open-chain skeletons) and 64-electron (square-planar skeletons) tetranuclear clusters, as well as different trinuclear clusters bearing P-bound exocyclic metal fragments. In most cases, these reactions also involve the cleavage of the P–P bond in the diphosphenyl ligand under mild conditions, to yield new phosphide (P) and phosphinidene (PMe) ligands displaying different coordination modes to three or four metal centers. Only on incorporation of the metal fragments  $MnCp'(CO)_2$  or  $W(CO)_5$  is the P–P bond of the diphosphenyl ligand preserved, this resulting in a novel, alkenyl-like,  $\mu\text{-}\kappa^2\text{:}\kappa^1\text{:}\kappa^1\text{:}\kappa^1$  coordination of the ligand to four metal centers.

## RESULTS AND DISCUSSION

**Tetranuclear Complexes Derived from Addition of 14- and 16-Electron Metal Fragments.** Compound **1** reacted readily with excess  $[Fe_2(CO)_9]$  (ca. 3 equiv) to give the tetranuclear phosphide- and phosphinidene-bridged derivative  $[Fe_2Mo_2Cp_2(\mu_4\text{-P})(\mu\text{-PCy}_2)(\mu_3\text{-PMe})(CO)_9]$  (**5**) (Chart 1), along with small amounts of the trinuclear cluster  $[FeMo_2Cp_2(\mu_3\text{-P})(\mu\text{-PCy}_2)(\mu_3\text{-PMe})(CO)_5]$  (**3a**). We recall here that compound **3a** was the major product in the reaction of **1** with stoichiometric amounts of  $[Fe_2(CO)_9]$  (Scheme 1).<sup>1</sup> Thus, it seems likely that **5** is formed upon reaction of **3a** with a second equivalent of  $[Fe_2(CO)_9]$ , as revealed through a separate experiment. This second step expectedly involves coordination of the 16-electron  $Fe(CO)_4$  fragment through the lone electron pair of the phosphide ligand present in **3a**.

In contrast, the reaction of **1** with excess  $[MnCp'(CO)_2(THF)]$  (ca. 4 equiv;  $Cp' = C_5H_4Me$ ) yielded

Chart 1



instead the tetranuclear diphosphenyl-bridged complex  $[Mn_2Mo_2Cp_2Cp'_2(\mu\text{-PCy}_2)(\mu\text{-}\kappa^2\text{:}\kappa^1\text{:}\kappa^1\text{:}\kappa^1\text{-P}_2Me)(CO)_6]$  (**6b**) (Chart 1), along with small amounts of the trinuclear complex  $[MnMo_2WCp_2(\mu\text{-PCy}_2)(\mu\text{-}\kappa^2\text{:}\kappa^1\text{-P}_2Me)(CO)_4]$  (**2b**) and substantial amounts of the phosphide-bridged derivative  $[MnMo_2Cp_2Cp'(\mu_3\text{-P})(\mu\text{-PCy}_2)(CO)_4]$  (**4b**) (typical ratio 3:1:3). Since our previous work revealed that **2b** is the major product in the reaction of **1** with stoichiometric amounts of  $[MnCp'(CO)_2(THF)]$ , while the phosphide complex **4b** follows from the thermal decomposition of **2b** in solution (Scheme 1),<sup>1</sup> then we can conclude that addition of the second  $MnCp'(CO)_2$  fragment on **2b** is not a particularly favored event. In fact, compound **6b** is rather unstable too, and also decomposed upon manipulation to give **4b** as the only carbonyl-containing product, possibly via Mn–P bond dissociation to regenerate **2b**.

The reaction of **1** with excess  $[W(CO)_5(THF)]$  (ca. 3.5 equiv) shares features with both reactions just discussed, since it leads to both diphosphenyl- and phosphide-bridged derivatives. Typically, a 3:2 mixture of the tetranuclear compounds  $[Mo_2W_2Cp_2(\mu\text{-PCy}_2)(\mu\text{-}\kappa^2\text{:}\kappa^1\text{:}\kappa^1\text{:}\kappa^1\text{-P}_2Me)(CO)_{12}]$  (**6d**) and  $[Mo_2W_2Cp_2(\mu_3\text{-P})(\mu\text{-PCy}_2)(\mu_3\text{-PMe})(CO)_{10}]$  (**7**) was obtained (Chart 1), along with small amounts of the known trinuclear phosphide-bridged complex  $[Mo_2WCp_2(\mu_3\text{-P})(\mu\text{-PCy}_2)(CO)_7]$  (**4d**) (Scheme 1). However, because of the relatively low reactivity of the tungsten adduct in THF, this reaction was better taken to completion by using toluene as solvent and by adding the adduct in two steps (see the Experimental Section).

The formation of compounds **6b,d** involves the addition of a second 16-electron  $ML_n$  fragment to a trinuclear intermediate of type **2** (Scheme 1) at the P atom of the PMe moiety, thus inducing the cleavage of one Mo–P(Me) bond. In contrast, the formation of compound **7** requires loss of two CO ligands from the Mo centers with concomitant P–P bond cleavage in the diphosphenyl ligand, which then yields phosphide and phosphinidene ligands bridging a Mo–Mo triple bond, according to the effective atomic number (EAN) formalism. Such a decarbonylation taking place at room temperature is highly unusual and can be only attributed to the presence of excess of the adduct  $[W(CO)_5(THF)]$  in solution, which

would act as an efficient CO trap (to give  $W(CO)_6$ ), thus triggering the P–P bond cleavage step that partially relieves the unsaturation generated by the loss of CO ligands at the Mo<sub>2</sub> center. This decarbonylation must take place at some intermediate stage of the reaction, since **6d** itself is not decarbonylated by  $[W(CO)_5(THF)]$ . Moreover, an independent experiment revealed that the Mo<sub>2</sub>( $\mu$ -PCy<sub>2</sub>)(CO)<sub>2</sub> core in compound **6d** was itself rather thermally robust in solution: upon refluxing a toluene solution of the complex for 1 h, only small amounts of **7** could be obtained, with the major product being the parent diphosphanyl complex **1**, obviously following from dissociation of the W(CO)<sub>5</sub> groups off the molecule. Surprisingly, in spite of the strong electronic unsaturation remaining at the dimetal center in **7**, exposure of the latter to a CO atmosphere did not result in the reverse carbonylation nor P–P coupling even under thermal activation (363 K) and moderate CO pressure ( $p_{CO}$  ca. 5 atm). The hypothetical transformation of **7** into **6d** would have been somehow reminiscent of the C–C coupling between carbyne ligands induced upon carbonylation of the related 30-electron complexes  $[Mo_2Cp_2(\mu-COMe)(\mu-CR)(\mu-PCy_2)]^+$  to give the corresponding alkyne-bridged derivatives  $[Mo_2Cp_2\{\mu-\eta^2:\eta^2-C_2R(OMe)\}(\mu-PCy_2)(CO)_2]^+$  (R = OMe, OEt,<sup>9</sup> Ph).<sup>10</sup>

Addition of the adduct  $[Mo(CO)_4(THF)_2]$  to solutions of **1** did not lead to the expected trinuclear compound  $[Mo_3Cp_2(\mu_3-P)(\mu-PCy_2)(\mu_3-PMe)(CO)_6]$  analogous to the tungsten complex **3d** (Scheme 1) but yielded instead complex reaction mixtures containing the tetranuclear cluster  $[Mo_4Cp_2(\mu_4-P)(\mu-PCy_2)(\mu_3-PMe)(CO)_9]$  (**8c**) (Chart 1), the known trinuclear complex  $[Mo_3Cp_2(\mu_3-P)(\mu-PCy_2)(CO)_7]$  (**4c**) (Scheme 1), and at least two other unidentified products. However, only the first two complexes could be isolated upon chromatographic workup of the mixture, with the tetranuclear **8c** being isolated in fair yield (ca. 60%). The presence of **4c** in the above mixtures can be accounted for by the action of  $[Mo(CO)_5(THF)]$ , always present in the solutions of  $[Mo(CO)_4(THF)_2]$ , which is known to react with **1** to give unstable intermediates eventually yielding the phosphide complex **4c**.<sup>1</sup> To explain the formation of **8c** one can envisage the addition of a Mo(CO)<sub>5</sub> fragment to the hypothetical complex  $[Mo_3Cp_2(\mu_3-P)(\mu-PCy_2)(\mu_3-PMe)(CO)_6]$  that would follow from the initial reaction of **1** with  $[Mo(CO)_4(THF)_2]$ . To check this mechanistic proposal, we carried out the reaction of the tungsten analogue  $[Mo_2WCp_2(\mu_3-P)(\mu-PCy_2)(\mu_3-PMe)(CO)_6]$  (**3d**) with  $[W(CO)_5(THF)]$  in toluene, which indeed yielded a related tetranuclear derivative  $[Mo_2W_2Cp_2(\mu_4-P)(\mu-PCy_2)(\mu_3-PMe)(CO)_9]$  (**8d**) in fair yield. The formation of complexes **8** also require full decarbonylation of the Mo<sub>2</sub>( $\mu$ -PCy<sub>2</sub>)(CO)<sub>2</sub> moiety at room temperature in the corresponding trinuclear precursors, as observed in the formation of **7**, an unusual process that we attribute once more to the CO-trapping action of the tetrahydrofuran adducts  $[M(CO)_{6-n}(THF)_n]$  ( $n = 1, 2$ ) used in these reactions.

#### Solid-State and Solution Structure of Compound 5.

The molecule of **5** in the crystal lattice (Figure 1 and Table 1) can be derived from that of its trinuclear precursor **3a** upon addition of a Fe(CO)<sub>4</sub> fragment to its phosphide ligand (P2) via the lone electron pair of the latter atom. All bond distances and angles within the former Mo<sub>2</sub>Fe trimetal moiety remain roughly unperturbed when compared to those in **3a**,<sup>1</sup> with the largest change probably being the elongation of some 0.07 Å in the Mo2–P2 distance, likely derived from increased steric pressure introduced by the added Fe(CO)<sub>4</sub> fragment, which

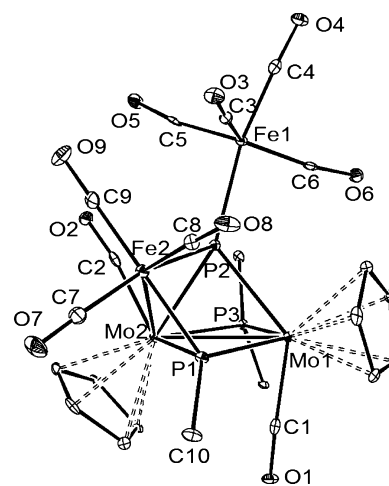


**Figure 1.** ORTEP diagram (30% probability) of compound **5** with H atoms and Cy groups (except the C<sup>1</sup> atoms) omitted for clarity.

**Table 1.** Selected Bond Lengths (Å) and Angles (deg) for Compound **5**

Mo1–Mo2	2.964(1)	C1–Mo1–Mo2	79.1(1)
Mo2–Fe2	2.935(1)	C2–Mo2–Mo1	118.8(1)
Mo1–P1	2.365(1)	P3–Mo1–P1	106.95(4)
Mo2–P1	2.452(1)	P2–Mo1–P1	66.58(4)
Mo1–P2	2.511(1)	P2–Mo1–P3	76.18(4)
Mo2–P2	2.543(1)	P1–Fe2–P2	73.76(5)
Mo1–P3	2.483(1)	Fe2–P2–Fe1	121.23(5)
Mo2–P3	2.497(1)	C7–Fe2–C8	100.6(2)
Fe1–P2	2.359(2)	C7–Fe2–C9	94.5(2)
Fe2–P2	2.285(1)	C8–Fe2–C9	101.0(2)
Fe2–P1	2.178(2)	P2–Fe1–C3	88.2(1)
Mo1–C1	1.986(5)	P2–Fe1–C4	167.7(1)
Mo2–C2	1.969(5)	C4–Fe1–C5	93.1(2)
P1–C10	1.832(4)	C6–Fe1–C5	121.8(2)

itself displays a slightly distorted trigonal bipyramidal environment, as expected. The length of 2.359(2) Å for the new exocyclic Fe1–P2 bond is consistent with the reference value of ca. 2.39 Å for a single Fe–P bond in a low-spin complex,<sup>11</sup> although it is significantly longer than the endocyclic Fe2–P2 length of 2.285(1) Å, possibly another effect of the mentioned steric congestion.

The most salient structural feature of **5**, however, is the coordination environment of its phosphide ligand. When bridging four metal atoms, phosphide ligands most commonly feature a tetrahedral environment. However, the environment around the P2 atom in **5** so much departs from tetrahedral that it might be better described as distorted trigonal pyramidal, with the P atom lying close (0.40 Å) to the Fe1Fe2Mo1 plane (base) and Mo2 acting as the apex of the pyramid. This environment is reminiscent of that commonly found in phosphinidene ligands bridging V-shaped trimetal cores (as it is indeed the case of P1, only 0.13 Å away from the Mo1Fe2C10 plane),<sup>12</sup> but has few precedents within the family of phosphide-bridged polynuclear complexes. Actually, only a few other phosphide complexes with a related P environment have been structurally characterized so far, most of them formally derived from the phosphide-bridged, V-shaped triiron anion  $[Fe_3(\mu_3-P)_2(CO)_9]^{2-}$ ,<sup>13–15</sup> along with the CrAu “star” complex  $[Au_3Cr_6(\mu_4-P)_3Cp_6(CO)_{12}]$ .<sup>16</sup>



Table 2. Selected IR<sup>a</sup> and <sup>31</sup>P{<sup>1</sup>H} NMR Data<sup>b</sup> for New Compounds

compound	$\nu(\text{CO})$	$\delta_{\text{P}}$ ( $J_{\text{PP}}$ ) [ $J_{\text{PW}}$ ]		
		PCy <sub>2</sub>	P	PMe
[Fe <sub>2</sub> Mo <sub>2</sub> Cp <sub>2</sub> ( $\mu_4$ -P)( $\mu$ -PCy <sub>2</sub> )( $\mu_3$ -PMe)(CO) <sub>9</sub> ] ( <b>5</b> )	2040 (vs), 2018 (s), 1972 (s), 1952 (m), 1919 (s)	129.8 (53, 10)	233.4 (191, 53)	272.5 (191, 10)
[Mn <sub>2</sub> Mo <sub>2</sub> Cp <sub>2</sub> Cp' <sub>2</sub> ( $\mu$ -PCy <sub>2</sub> )( $\mu_4$ -P <sub>2</sub> Me)(CO) <sub>6</sub> ] ( <b>6b</b> )		121.1 <sup>c</sup>	-5.4 (br) (ca. 500) <sup>c</sup>	143.9 (br) (ca. 500) <sup>c</sup>
[Mo <sub>2</sub> W <sub>2</sub> Cp <sub>2</sub> ( $\mu$ -PCy <sub>2</sub> )( $\mu_4$ -P <sub>2</sub> Me)(CO) <sub>12</sub> ] ( <b>6d</b> )	2067 (w), 2060 (w), 1974 (w, sh), 1956 (m, sh), 1934 (vs), 1922 (s, sh)	153.4 (9)	-116.5 (431) [238]	93.9 (431, 9) [193]
[Mo <sub>2</sub> W <sub>2</sub> Cp <sub>2</sub> ( $\mu_3$ -P)( $\mu$ -PCy <sub>2</sub> )( $\mu_3$ -PMe)(CO) <sub>10</sub> ] ( <b>7</b> )	2065 (w), 2053 (m), 1944 (vs), 1923 (s)	293.2 (24, 12)	941.8 (24, 19) [166]	340.6 (19, 12) [190]
[Mo <sub>4</sub> Cp <sub>2</sub> ( $\mu_4$ -P)( $\mu$ -PCy <sub>2</sub> )( $\mu_3$ -PMe)(CO) <sub>9</sub> ] ( <b>8c</b> )	2061 (m), 2011 (vs), 1944 (s), 1916 (m)	178.3 (26, 7)	663.7 (br)	397.9 (26, 7)
[Mo <sub>2</sub> W <sub>2</sub> Cp <sub>2</sub> ( $\mu_4$ -P)( $\mu$ -PCy <sub>2</sub> )( $\mu_3$ -PMe)(CO) <sub>9</sub> ] ( <b>8d</b> )	2060 (m), 2011 (vs), 1940 (vs), 1911 (s)	167.0 (32, 7)	554.6 (br) [253, 187]	363.7 (32, 3)
[Mn <sub>2</sub> Mo <sub>2</sub> Cp <sub>2</sub> ( $\mu_4$ -P)( $\mu$ -PCy <sub>2</sub> )( $\mu_3$ -PMe)(CO) <sub>9</sub> ] ( <b>9e</b> )	2053 (s), 1982 (m, sh), 1970 (s), 1962 (vs), 1934 (w), 1912 (m), 1883 (w, sh)	125.3 (85, 18)	419.6 (306, 85)	133.7 (306, 18)
[Mo <sub>2</sub> Re <sub>2</sub> Cp <sub>2</sub> ( $\mu_4$ -P)( $\mu$ -PCy <sub>2</sub> )( $\mu_3$ -PMe)(CO) <sub>9</sub> ] ( <b>9f</b> )	2076 (m), 1988 (vs), 1973 (m, sh), 1932 (w), 1915 (m), 1882 (w)	120.4 (91, 12)	208.7 (229, 91)	18.9 (229, 12)
[Co <sub>2</sub> Mo <sub>2</sub> Cp <sub>2</sub> ( $\mu_4$ -P)( $\mu$ -PCy <sub>2</sub> )( $\mu_4$ -PMe)( $\mu$ -CO)(CO) <sub>6</sub> ] ( <b>10</b> )	2023 (vs), 1994 (s), 1964 (m), 1891 (m), 1877 (w, sh), 1821 (w)	184.9 (9, 9)	178.6 (br) (42)	208.1 (42, 9)

<sup>a</sup>Recorded in dichloromethane solution, with C–O stretching bands [ $\nu(\text{CO})$ ] in cm<sup>-1</sup>. <sup>b</sup>Recorded in CD<sub>2</sub>Cl<sub>2</sub> at 121.50 MHz and 298 K, with coupling constants ( $J_{\text{PP}}$ ) and [ $J_{\text{PW}}$ ] in Hz. <sup>c</sup>In tetrahydrofuran solution, at 162.14 MHz.

Spectroscopic data in solution for **5** are fully consistent with the solid-state structure discussed above. Its IR spectrum in dichloromethane solution (Table 2) displays five strong bands at frequencies well over 1900 cm<sup>-1</sup> that can be safely identified as a superimposition of bands arising from the relatively independent Fe(CO)<sub>3</sub> and Fe(CO)<sub>4</sub> oscillators of the molecule.<sup>17</sup> C–O stretches arising from the transoid Mo<sub>2</sub>(CO)<sub>2</sub> oscillator are expected to be of weaker intensity and lower energy,<sup>1</sup> and in the case of **5** these can be only detected when recording the IR spectrum in the solid state (a medium-intensity band at 1890 cm<sup>-1</sup> is then observed, which can be assigned to the Mo<sub>2</sub>(CO)<sub>2</sub> oscillator; see the Experimental Section).

The <sup>31</sup>P{<sup>1</sup>H} NMR spectrum of **5** exhibits three doublets of doublets at 272.5, 233.4, and 129.8 ppm corresponding to the phosphinidene (PMe), phosphide (P), and PCy<sub>2</sub> ligands, respectively. These shifts are comparable to those in the trinuclear precursor **3a**, which is a bit surprising in the case of the phosphide resonance (shifted by only ca. 6 ppm) if we take into account the strong modification operated on its chemical environment (from  $\mu_3$  to  $\mu_4$  coordination). In contrast, there is a huge increase in the absolute values of the two-bond P–P couplings for the phosphide ligand when going from **3a** (ca. 0 Hz coupling with PMe and 9 Hz with PCy<sub>2</sub>) to **5** (191 Hz with PMe and 53 Hz with PCy<sub>2</sub>). This dramatic change can be related in part to the disappearance of the large contribution to the P–P coupling imposed by the presence of a lone electron pair on the phosphide ligand in **3a**.<sup>18</sup> In the absence of such disturbing effect, large P–P couplings should be then expected for **5** by considering the quite acute angles defined by the P–M–P paths connecting the phosphide ligand with the PMe (average 68° for three paths) and PCy<sub>2</sub> (average 76° for two paths) ligands in this molecule.<sup>19</sup> As it will be discussed below, the structurally related compounds **9e,f** display even higher <sup>2</sup> $J_{\text{PP}}$  values that can be related with even more acute P–M–P angles. We can also quote here the pentanuclear cluster [Fe<sub>5</sub>Cp-(C<sub>5</sub>Me<sub>5</sub>)( $\mu_4$ -P)<sub>2</sub>(CO)<sub>13</sub>], a molecule having inequivalent  $\mu_4$ -P ligands with environments comparable to that of **5**, which also displays a high two-bond P–P coupling of 140 Hz (two P–Fe–P paths of 74°).<sup>14</sup>

The <sup>1</sup>H and <sup>13</sup>C{<sup>1</sup>H} NMR spectra of **5** display in general the number of resonances expected for a molecule devoid of any symmetry elements, with the exception of the resonances of Fe-bound carbonyls (see the Experimental Section). Thus, at room temperature only an averaged doublet resonance at 215.6 ppm was observed in the <sup>13</sup>C NMR spectrum, which is assigned to an Fe(CO)<sub>3</sub> moiety undergoing fast rotational exchange of the carbonyl sites on the NMR time scale, whereas no resonances were detected for the Fe(CO)<sub>4</sub> group, probably lost in the baseline due to dynamic effects. Indeed, the 220 K spectrum of this complex displayed two new resonances: a broad one at 209.4 ppm assigned to the three equatorial CO ligands of the Fe(CO)<sub>4</sub> fragment, and a doublet at 216.4 ppm ( $J_{\text{CP}} = 13$  Hz) assigned to its axial CO ligand.

**Solid-State Structure of Compound 6d.** The molecule of **6d** in the crystal (Figure 2 and Table 3) is built from two

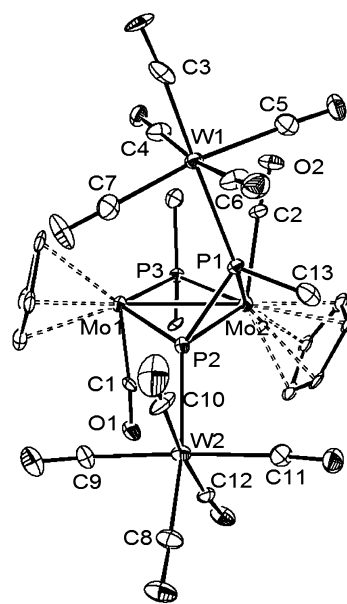


Figure 2. ORTEP diagram (30% probability) of compound **6d** with H atoms and Cy groups (except the C<sup>1</sup> atoms) omitted for clarity.

**Table 3.** Selected Bond Lengths (Å) and Angles (deg) for Compound **6d**

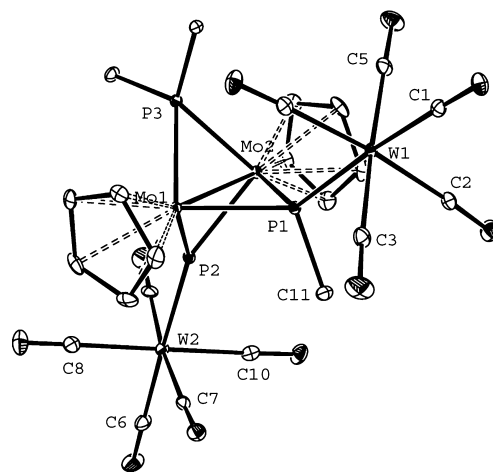
Mo1–Mo2	2.760(2)	C1–Mo1–Mo2	83.1(5)
Mo1–P2	2.414(4)	C2–Mo2–Mo1	97.7(5)
Mo2–P2	2.508(5)	P3–Mo1–P2	113.5(2)
Mo2–P1	2.640(5)	P3–Mo2–P2	108.2(2)
Mo1–P3	2.386(5)	P1–Mo2–P3	124.3(2)
Mo2–P3	2.445(4)	W1–P1–P2	127.2(2)
P1–P2	2.097(7)	C13–P1–W1	109.4(8)
W1–P1	2.539(4)	C13–P1–P2	108.9(8)
W2–P2	2.564(5)	W2–P2–P1	122.6(2)
Mo1–C1	1.95(2)	P1–W1–C3	178.6(7)
Mo2–C2	2.05(2)	P1–W1–C7	89.1(7)
P1–C13	1.85(2)	P2–W2–C8	173.7(7)
		P2–W2–C9	87.1(6)

MoCp(CO) units in a transoid arrangement bridged rather symmetrically by a PCy<sub>2</sub> ligand, and asymmetrically by a diphosphenyl ligand that bears exocyclic W(CO)<sub>5</sub> fragments on each P atom, thus rendering an overall  $\mu_4\text{-}\kappa^2\text{:}\kappa^1\text{:}\kappa^1\text{:}\kappa^1$  coordination mode for this ligand. To our knowledge, this is the first reported example of a diphosphenyl complex displaying such coordination mode, and actually we are only aware of just another structurally characterized complex having a  $\mu_4\text{-P}_2\text{R}$  ligand at all, this being the tetrairon cluster [Fe<sub>4</sub>(CO)<sub>10</sub>( $\mu_4\text{-PPh}$ )( $\mu_4\text{-P}_2\text{Ph}$ )( $\mu\text{-PPh}_2$ )], which displays a diphosphenyl ligand symmetrically bridging a Fe<sub>4</sub> square planar core in a  $\mu_4\text{-}\kappa^1\text{:}\kappa^1\text{:}\kappa^1\text{:}\kappa^1$  fashion.<sup>20</sup> When compared with the parent complex **1**, the diphosphenyl coordination to the Mo<sub>2</sub> unit in **5** has been modified not only by the removal of one of the Mo–P(Me) bonds but also in its relative disposition with respect to the PCy<sub>2</sub> ligand. Thus, the P atom (P2), formerly placed in an “apical” position (*cis* with respect to the PCy<sub>2</sub> ligand in **1**), is now placed in the “basal” position (close to the Mo<sub>2</sub>PCy<sub>2</sub> plane) and bridges the Mo<sub>2</sub> unit asymmetrically (ca. 0.1 Å closer to Mo1); in contrast, the PMe atom (P1), formerly placed in a basal position, is now placed well above that plane and just bound to the Mo2 atom. Each of these P atoms is further bound to an exocyclic W(CO)<sub>5</sub> fragment with P–W distances (ca. 2.55 Å) comparable to that one in the complex [W(CO)<sub>5</sub>(PPh<sub>3</sub>)] (2.545(1) Å),<sup>21</sup> which gives support to the formulation of dative single P→W bonds under conditions of significant steric pressure. Then, by recalling the isolobal analogy between P→W(CO)<sub>5</sub> and CR fragments,<sup>1</sup> the coordination of the WP–P(Me)W moiety to the Mo<sub>2</sub> subunit might be related to that of  $\sigma,\pi$ -bound alkenyl ligands in related compounds such as [Mo<sub>2</sub>Cp<sub>2</sub>( $\mu\text{-}\eta^1\text{:}\eta^2\text{-CMe=CHMe}$ )( $\mu\text{-SPh}$ )(CO)<sub>2</sub>],<sup>22</sup> and [Mo<sub>2</sub>Cp<sub>2</sub>( $\mu\text{-}\eta^1\text{:}\eta^2\text{-CH=CH}_2$ )( $\mu\text{-PCy}_2$ )(CO)<sub>3</sub>].<sup>23</sup> Interestingly, the P–P distance of 2.097(7) Å in **6d** still is ca. 0.11 Å shorter than the interatomic separation in the P<sub>4</sub> molecule (2.21 Å), thus suggesting the presence of some residual  $\pi$ (P–P) contribution to that bond. The alkenyl analogy also implies a formal electron count of 32 electron for the Mo<sub>2</sub> center in **6d**, and therefore leads to the formulation of an intermetallic double bond, which is consistent with the Mo–Mo separation of 2.760(2) Å, only slightly longer than the reference distance of ca. 2.71 Å in *trans*-[Mo<sub>2</sub>Cp<sub>2</sub>( $\mu\text{-PPh}_2$ )<sub>2</sub>(CO)<sub>2</sub>],<sup>24</sup> but much shorter (by ca. 0.25 Å) than the intermetallic separation in the electron-precise parent diphosphenyl complex **1** (3.0172(4) Å), a molecule with a Mo–Mo single bond.<sup>4</sup>

**Solution Structure of Compounds 6b,d.** Spectroscopic data in solution for **6d** are in fairly good agreement with the structure found in the solid state. Its IR spectrum in dichloromethane solution displays six bands at frequencies above 1900 cm<sup>−1</sup> due to the C–O stretches of W-bound carbonyls, with the appearance of two high-frequency bands at ~2060 cm<sup>−1</sup> being indicative of the presence of two pentacarbonyl oscillators in the molecule.<sup>17</sup> Its <sup>31</sup>P{<sup>1</sup>H} NMR spectrum displays two strongly coupled resonances (<sup>1</sup>J<sub>PP</sub> = 431 Hz) for the diphosphenyl ligand, at −116.5 and 93.9 ppm, which can be unambiguously assigned to the P and PMe groups, respectively, after comparison with the corresponding <sup>1</sup>H-coupled <sup>31</sup>P NMR spectrum (see the Experimental Section). Both resonances are some 180 ppm more deshielded than the corresponding resonances in the parent compound **1** as a result of coordination to W(CO)<sub>5</sub> fragments, and display <sup>31</sup>P–<sup>193</sup>W couplings of ca. 200 Hz as expected, while the retention of a large P–P coupling is consistent with the short P–P bond length measured in the crystal.

As noted above, we could not isolate the unstable dimanganese complex **6b**, and only limited spectroscopic data could be obtained for this molecule. For instance, unambiguous assignment of the corresponding C–O stretching bands could not be done due to overlapping with those of compounds **2b** and **4b** invariably present in the crude reaction mixtures. Even so, its <sup>31</sup>P{<sup>1</sup>H} NMR spectrum supports a structure analogous to that of **6d**, since it displays a pair of strongly coupled resonances at 143.9 and −5.4 ppm (<sup>1</sup>J<sub>PP</sub> ca. 500 Hz), a circumstance clearly indicative of the retention of the P–P bond in the diphosphenyl ligand. The assignment of these resonances to each of the P atoms of the ligand could not be made unambiguously due to their broadness (in turn derived from their coordination to the quadrupolar <sup>55</sup>Mn nuclei), but their identification as PMe and P resonances, respectively (based on the assignment of the ditungsten complex **6d**), leads to overall deshieldings of ca. 260–290 ppm relative to the parent complex **1**, which seems a reasonable deshielding effect for coordination of a first-row transition metal fragment to the corresponding phosphorus atoms, even if a bit more modest than anticipated.

**Solid-State and Solution Structure of Compound 7.** The central core of the molecule (Figure 3 and Table 4) is built

**Figure 3.** ORTEP diagram (30% probability) of compound **7** with H atoms and Cy groups (except the C<sup>1</sup> atoms) omitted for clarity.

**Table 4.** Selected Bond Lengths (Å) and Angles (deg) for Compound 7

Mo1–Mo2	2.5542(4)	P3–Mo1–P1	93.86(2)
Mo1–P1	2.4288(6)	P2–Mo1–P1	92.61(2)
Mo2–P1	2.4248(7)	P3–Mo1–P2	94.70(2)
Mo1–P2	2.2938(7)	W1–P1–C11	108.96(8)
Mo2–P2	2.3110(6)	P1–W1–C1	175.97(7)
Mo1–P3	2.4000(6)	P1–W1–C2	86.12(7)
Mo2–P3	2.3859(7)	P2–W2–C6	178.36(7)
W1–P1	2.5286(7)	P2–W2–C7	86.45(7)
W2–P2	2.4555(7)	Mo1–P2–W2	142.50(3)
P1–C11	1.851(2)	Mo2–P2–W2	148.55(3)
		Mo1–P2–Mo2	63.51(2)

from two MoCp fragments symmetrically bridged by three P-donor ligands in a “Y” disposition around the Mo–Mo vector (PMo<sub>2</sub>P torsion angles ca. 120°): dicyclohexylphosphide, phosphide, and a methylphosphinidene, with the latter two ligands further coordinated to an exocyclic W(CO)<sub>5</sub> moiety each. The corresponding P→W lengths now are significantly different, with a more reduced value of 2.456(1) Å for the W2–P2 bond, likely reflecting the smaller steric congestion around the trigonal-planar phosphide P2 atom (cf. 2.457(3) Å in the phosphide-bridged complex **4d**).<sup>1</sup> The Mo–P lengths for the three bridging ligands are significantly different from each other, with the values of ca. 2.42 Å ( $\mu_3$ -PMe), 2.40 Å ( $\mu$ -PCy<sub>2</sub>) and 2.30 Å ( $\mu_3$ -P) reflecting the different bonding interactions involved. Thus, the longer values observed for the phosphinidene ligand are consistent with its formal contribution of two electrons to the dimetal center and subsequent formulation of single Mo–P bonds. On the other extreme, an order of 1.5 must be formulated for the Mo–P bonds of the trigonal planar phosphide ligand, due to the presence of a  $\pi$ -bonding interaction expected to be delocalized over the Mo<sub>2</sub>P triangle, as supported by density functional theory calculations on the related phosphide-bridged complex **4d** (Mo–P 2.30 Å).<sup>1</sup> Indeed these short distances turn out to be nearly identical to those measured in the trigonal phosphinidene complexes [Mo<sub>2</sub>Cp<sub>2</sub>( $\mu$ -PMes\*)(CO)<sub>4</sub>],<sup>25</sup> and [Mo<sub>2</sub>Cp<sub>2</sub>( $\mu$ -PMes\*)( $\mu$ -CO)<sub>2</sub>],<sup>26</sup> for which analogous Mo–P bond orders are to be proposed.

The dimolybdenum unit in **7** bears just 30 valence electrons, and therefore a Mo–Mo triple bond should be formulated for this molecule according to the EAN formalism, which is fully consistent with the very short intermetallic distance of 2.5542(4) Å, not far from the reference value of 2.515(2) Å measured for the related complex [Mo<sub>2</sub>Cp<sub>2</sub>( $\mu$ -PPh<sub>2</sub>)<sub>2</sub>( $\mu$ -CO)].<sup>24</sup> By using the isolobal analogy between P→W(CO)<sub>5</sub> and CR fragments,<sup>1</sup> we can also relate complex **7** with the 30-electron carbyne complexes of the type [Mo<sub>2</sub>Cp<sub>2</sub>( $\mu$ -CX)( $\mu$ -PCy<sub>2</sub>)( $\mu$ -CO)] (X = H, Ph, OMe, OEt), which indeed display comparable structures, although with shorter Mo–Mo lengths of ca. 2.47 Å, due to the lower covalent radii of the bridging C atoms implied.<sup>27</sup>

Spectroscopic data in solution for **7** are fully consistent with the structure in the crystal. Of particular interest is its <sup>31</sup>P{<sup>1</sup>H} NMR spectrum, which displays a highly deshielded resonance at 941.8 ppm, a characteristic signature for trigonal planar  $\mu_3$ -P ligands,<sup>1</sup> along with resonances at 340.6 and 293.2 ppm corresponding to the  $\mu_3$ -PMe and PCy<sub>2</sub> ligands, respectively. The chemical shift of the latter resonance is much higher than the corresponding ones in the parent complex **1** ( $\delta_p$  156 ppm)

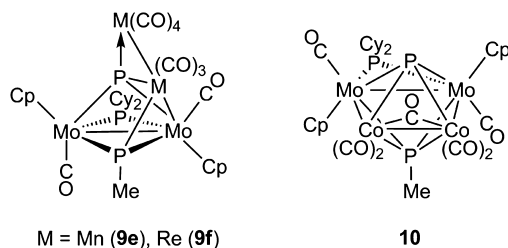
and all other compounds reported in this work (Table 2) but falls in the range observed for structurally related compounds bearing PCy<sub>2</sub> groups bridging over Mo–Mo triple bonds, such as the diorganophosphide complexes [Mo<sub>2</sub>Cp<sub>2</sub>( $\mu$ -PCy<sub>2</sub>)( $\mu$ -PRR')( $\mu$ -CO)] ( $\delta_p$  ca. 240 ppm),<sup>28</sup> the phosphide complex [Mo<sub>2</sub>WCp<sub>2</sub>( $\mu_3$ -P)( $\mu$ -PCy<sub>2</sub>)( $\mu$ -CO)(CO)<sub>5</sub>] (246.0 ppm),<sup>1</sup> or the methylidyne complex [Mo<sub>2</sub>Cp<sub>2</sub>( $\mu$ -CH)( $\mu$ -PCy<sub>2</sub>)( $\mu$ -CO)] (288.2 ppm).<sup>29</sup> Moreover, <sup>2</sup>J<sub>PP</sub> values measured for **7** (in the range of 12–24 Hz) are comparable to those found in the mentioned diorganophosphide complexes, as expected from the comparable values of the corresponding P–Mo–P angles involved (~90°). The <sup>1</sup>H and <sup>13</sup>C{<sup>1</sup>H} NMR spectra of **7** display the expected number of resonances considering the symmetry of the molecule and deserve no particular comments.

**Structure of Compounds 8c,d.** Unfortunately, crystals suitable for an X-ray analysis of these compounds could not be grown, but the available spectroscopic data in solution give solid support to the structure proposed for these molecules (Chart 1). The IR spectra of these compounds exhibit four bands as in compound **7**, but now those bands above 2000 cm<sup>-1</sup>, corresponding to the symmetrical stretches of the M(CO)<sub>x</sub> fragments, have very different frequencies and can be safely attributed to the presence of M(CO)<sub>5</sub> (ca. 2060 cm<sup>-1</sup>) and M(CO)<sub>4</sub> (2011 cm<sup>-1</sup>) oscillators in the molecule.<sup>17</sup> The <sup>31</sup>P{<sup>1</sup>H} NMR spectra of these compounds display three distinct resonances in each case, and the most deshielded one (663.7 ppm in **8c** and 554.6 ppm in **8d**) corresponds to a phosphide ligand, with that of the ditungsten compound expectedly displaying two sets of satellite signals due to one-bond coupling to inequivalent W nuclei (<sup>1</sup>J<sub>PP</sub> = 225 and 183 Hz). We note that the chemical shift of these phosphide resonances is higher than anticipated for a  $\mu_4$ -P ligand in a tetrahedral environment (cf. 279.3 ppm for the related cluster [MoW<sub>3</sub>CpCp\*( $\mu_2$ -O)( $\mu_4$ -P)<sub>2</sub>(CO)<sub>14</sub>]),<sup>30</sup> perhaps an effect of the electronic unsaturation of the Mo<sub>2</sub>W core of these molecules. In contrast, the phosphinidene and PCy<sub>2</sub> resonances display unremarkable chemical shifts and P–P couplings. On the other hand, the <sup>1</sup>H and <sup>13</sup>C{<sup>1</sup>H} NMR spectra are consistent with the presence in these molecules of a symmetry plane containing all three P atoms and rendering equivalent chemical environments for the MoCp fragments. As expected, the <sup>13</sup>C{<sup>1</sup>H} NMR spectrum of **8d** displays no resonances corresponding to Mo-bound carbonyls but just a resonance at 200.1 ppm corresponding to the equatorial carbonyls of the W(CO)<sub>5</sub> fragment and a resonance at 213.2 ppm corresponding to the W(CO)<sub>4</sub> group, with the latter indicating fast rotational exchange even at 213 K.

**Reactions of 1 with Metal Carbonyl Dimers [M<sub>2</sub>(CO)<sub>n</sub>] (M = Mn, Re, Co; n = 10, 8).** These reactions led invariably to the cleavage of the P–P bond in the diphosphenyl ligand to give novel phosphide- and phosphinidene-bridged tetranuclear clusters incorporating a partially decarbonylated dimetal moiety, with preservation of the corresponding M–M bond (Chart 2). Reactions with the manganese and rhenium dimers [M<sub>2</sub>(CO)<sub>10</sub>] took only place under UV–visible irradiation to give the open-chain 66-electron tetranuclear clusters [M<sub>2</sub>Mo<sub>2</sub>Cp<sub>2</sub>( $\mu_4$ -P)( $\mu$ -PCy<sub>2</sub>)( $\mu_3$ -PMe)(CO)<sub>9</sub>] (M = Mn (**9e**), Re (**9f**)), involving the formation of just one new Mo–M bond. In contrast, compound **1** reacted at room temperature with a slight excess of the cobalt dimer [Co<sub>2</sub>(CO)<sub>8</sub>] to give the square planar 64-electron cluster [Co<sub>2</sub>Mo<sub>2</sub>Cp<sub>2</sub>( $\mu_4$ -P)( $\mu$ -PCy<sub>2</sub>)( $\mu_4$ -PMe)( $\mu$ -CO)(CO)<sub>6</sub>] (**10**) in good yield, which implies the formation of two new Mo–Co bonds. Although a dimetal

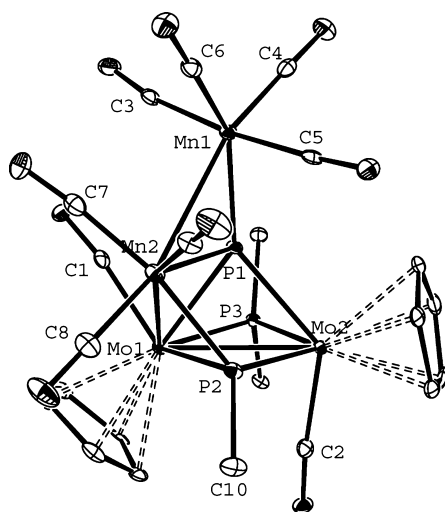


Chart 2



moiety is formally added to the diphosphenyl complex **1** in all the above reactions, it is very unlikely that the latter proceed at all in a single step, but most probably involve the successive addition of 17-electron mononuclear radicals  $M(\text{CO})_5$  and  $\text{Co}(\text{CO})_4$  intermingled with several decarbonylation steps. However, no intermediate species were detected when monitoring the above reactions by IR and  $^{31}\text{P}$  NMR spectroscopy, and the exact sequence of events in these complex reactions is unknown.

**Solid-State Structure of Compounds 9e,f.** The molecular structures of both compounds were determined through an X-ray analysis and were found to be very similar to each other, except for differences expected from the distinct covalent radii of manganese and rhenium; a drawing of the manganese compound is shown in Figure 4, while the main geometrical



**Figure 4.** ORTEP diagram (30% probability) of compound **9e** with H atoms and Cy groups (except the  $\text{C}^1$  atoms) omitted for clarity.

parameters for both compounds are collected in Table 5. These molecules can be formally derived from the structure of compound **5** after replacement of Fe with Mn (or Re) atoms and creation of an intermetallic bond linking the  $M(\text{CO})_4$  and  $M(\text{CO})_3$  units, with M–M distances of 2.9286(8) Å (Mn) and 3.1003(4) Å (Re) not far from the corresponding values in the parent  $[\text{M}_2(\text{CO})_{10}]$  complexes (2.9038(6) and 3.041(1) Å, respectively),<sup>31</sup> while the Mo–Mo and Mo–M lengths also are as expected for single bonds. The metal–P distances display considerable variations depending on the identity and electronic needs of the different metal fragments of the molecule, but they all have values consistent with the presence of single bonds too. We note, however, the reduced values for the M1–P1 and M2–P2 bonds (of ca. 2.23 and 2.38 Å for Mn and Re bonds, respectively), which are some 0.1 Å shorter than

the corresponding M2–P1 bond and approach the figures usually observed for dative  $\text{P} \rightarrow \text{M}$  bonds in comparable metal fragments under conditions of low steric pressure (cf. 2.2326(7) Å in  $ax\text{-}[\text{Mn}_2(\text{CO})_9(\text{PPhC}_8\text{H}_6)]$ ,<sup>32</sup> and 2.328(1) Å in  $ax\text{-}[\text{Re}_2(\text{CO})_9\{\text{P}(\text{C}_4\text{H}_3\text{O})_3\}]$ .<sup>33</sup> From this we can conclude that the phosphide and phosphinidene ligands formally act as two-electron donors to the M1 and M2 atoms, respectively, and as one-electron donors to all other metal atoms to which they are bound.

The presence of the M–M bond in the structure of complexes **9** has the structural effect (when compared to that in **5**) of further forcing distortion on the phosphide environment away from tetrahedral, to the point that the P1 atom is now placed only 0.09 Å off the plane defined by the Mo1, Mo2, and M1 atoms, to render a trigonal pyramidal-like environment, with the M2 atom acting as the apex. As noted when discussing the structure of **5**, this environment around a phosphide ligand has a few precedents. We also note that in compounds **5** and **9** the phosphide ligand is providing in each case a total of five electrons to the four metal centers bound to it; therefore, there is no electron density available to occupy the space opposite the apex of the distorted pyramid surrounding the P atom, which then likely might behave as an electrophilic site of the molecule, a matter to be addressed through future investigations.

**Solution Structure of Compounds 9e,f.** The available spectroscopic data in solution for the title compounds (Table 2 and Experimental Section) are in good agreement with their solid-state structures. Their IR spectra exhibit several bands above  $1900\text{ cm}^{-1}$ , six for **9e** and five for **9f**, which can be safely assigned to C–O stretches of the  $M(\text{CO})_4$  and  $M(\text{CO})_3$  fragments. In both spectra, a weak band at ca.  $1880\text{ cm}^{-1}$  can be attributed to Mo-bound CO ligands. In addition, the spectra recorded in Nujol mulls for these species display two bands below  $1900\text{ cm}^{-1}$  of medium and strong intensities in order of decreasing frequencies, in better agreement with the presence of a transoid  $\text{Mo}_2(\text{CO})_2$  oscillator in these molecules.

The most remarkable feature in the  $^{31}\text{P}\{^1\text{H}\}$  NMR spectra of these complexes is the high  $^2J_{\text{PP}}$  couplings involving the phosphide ligand, of 306 (**9e**) or 229 Hz (**9f**) with the phosphinidene ligand and ca. 90 Hz with the  $\text{PCy}_2$  ligand. These values are even higher than the corresponding couplings measured for compound **5** (191 and 53 Hz) and can be in part explained on the basis of the lower P–M–P angles involved (for instance, the average angles are ca. 63 (**9e**), 64 (**9f**), and 68° (**5**) for the three P–M–P paths connecting the P and  $\text{PMe}$  ligands). In addition, by considering the relatively short separations of 2.51 (**9e**) and 2.59 Å (**9f**) between these P atoms in the crystal (Table 5), we cannot exclude the contribution of some residual P–P bonding interaction to this coupling. Indeed, P–P bonds can be established at quite long distances (2.50–2.70 Å), as found for several asymmetric and sterically encumbered diphosphines.<sup>34</sup> On the other hand, we note that the phosphide ligand in our compounds is substantially more deshielded (by ca. 190 ppm) than the corresponding phosphinidene ligand, whereas the opposite trend was observed in compound **5**, a difference that might be related to the stronger distortion, away from the tetrahedral environment, of the phosphide ligands in compounds **9**. We finally note that the chemical shifts of these ligands are much lower when bound to Re rather than to the light Mn atom, as anticipated.<sup>35</sup> Expectedly, this difference is almost doubled for the phosphide atom (ca. 210 ppm more deshielded for **9e**) compared to the phosphinidene atom (ca. 110 ppm more

Table 5. Selected Bond Lengths (Å) and Angles (deg) for Compounds 9e (M = Mn) and 9f (M = Re)<sup>a</sup>

parameter	9e	9f	parameter	9e	9f
Mo1–Mo2	2.9674(5)	2.9585(4)	C1–Mo1–Mo2	123.2(1)	122.6(1)
Mo1–M2	2.9988(7)	3.1003(4)	C2–Mo2–Mo1	80.1(1)	80.3(1)
M1–M2	2.9286(8)	3.0915(2)	P1–Mo1–P3	72.90(3)	72.52(3)
Mo1–P1	2.4474(9)	2.4521(9)	P1–Mo1–P2	60.85(3)	62.40(3)
Mo2–P1	2.462(1)	2.466(1)	P2–Mo1–P3	103.38(3)	103.45(3)
M1–P1	2.227(1)	2.3672(9)	Mo1–P1–Mo2	74.38(3)	73.96(3)
M2–P1	2.334(1)	2.4738(9)	Mo1–P1–M1	142.99(5)	142.69(4)
Mo1–P2	2.513(1)	2.549(1)	Mo2–P1–M1	142.09(4)	142.79(4)
Mo2–P2	2.402(1)	2.405(1)	M1–P1–M2	79.85(4)	79.34(3)
M2–P2	2.247(1)	2.383(1)	P1–M2–P2	66.49(4)	64.48(3)
Mo1–P3	2.445(1)	2.4433(9)	C3–M1–C4	86.5(2)	86.6(2)
Mo2–P3	2.500(1)	2.501(1)	C3–M1–C5	173.6(2)	174.4(2)
Mo1–C1	1.961(4)	1.958(4)	C4–M1–C6	100.2(2)	96.7(2)
Mo2–C2	1.996(4)	1.993(4)	C7–M2–C8	89.4(2)	90.4(2)
P2–C10	1.841(4)	1.842(4)	C7–M2–M1	76.2(1)	76.0(1)
P1...P2	2.513(1)	2.592(1)	C5–M1–M2	86.7(1)	86.7(1)

<sup>a</sup>Values according to the labeling of Figure 4.

deshielded for 9e) in agreement with the number of group 7 atoms bound to them (two and one, respectively).

#### Solid-State and Solution Structure of Compound 10.

The molecule of 10 in the crystal (Figure 5 and Table 6)

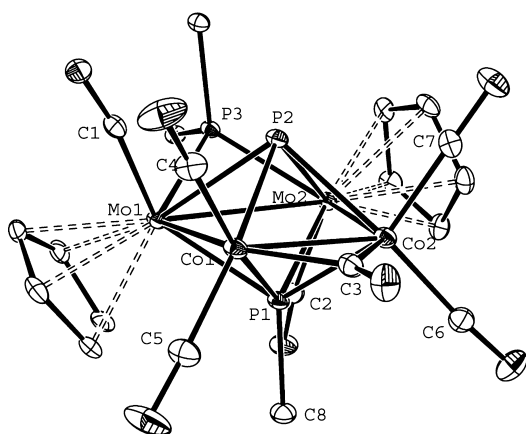


Figure 5. ORTEP diagram (30% probability) of compound 10 with H atoms and Cy groups (except the C<sup>1</sup> atoms) omitted for clarity.

displays a square planar Mo<sub>2</sub>Co<sub>2</sub> core symmetrically capped by methylphosphinidene and phosphide ligands, to render an overall octahedral M<sub>4</sub>P<sub>2</sub> core further bridged by a PCy<sub>2</sub> ligand symmetrically placed on the Mo–Mo edge, coplanar with the Mo<sub>2</sub>P(Me) triangle, and by a CO ligand symmetrically placed over the Co–Co edge and coplanar with the metal atoms. The coordination sphere of the Mo<sub>2</sub> unit is completed by terminal Cp and CO ligands in a distorted transoid arrangement, while that of the Co<sub>2</sub> unit is completed with two terminal CO ligands in each case. The structure thus can be formally derived from that of the parent compound 1 upon insertion of a Co<sub>2</sub>(CO)<sub>5</sub> moiety to build the metal square with full cleavage of the diphosphenyl P–P bond, which then yields P and PMe ligands capping on opposite sides of the metal core. All intermetallic distances are consistent with the formulation of single metal–metal bonds in each case, after considering the different covalent radii of Mo and Co,<sup>11</sup> and the geometrical parameters involving the Co<sub>2</sub>(μ-CO)(CO)<sub>4</sub> subunit are comparable to those measured for the large family of structurally related

Table 6. Selected Bond Lengths (Å) and Angles (deg) for Compound 10

Mo1–Mo2	3.0812(4)	C1–Mo1–Mo2	114.5(1)
Mo1–Co1	2.8812(7)	C2–Mo2–Mo1	80.9(1)
Mo2–Co2	2.9067(7)	P1–Mo1–P2	63.15(3)
Co1–Co2	2.5008(8)	P1–Mo1–P3	102.18(3)
Mo1–P1	2.442(1)	P2–Mo1–P3	72.22(3)
Mo2–P1	2.475(1)	Mo1–Mo2–Co2	83.72(2)
Co1–P1	2.256(1)	Mo2–Co2–Co1	95.77(2)
Co2–P1	2.210(1)	Co2–Co1–Mo1	95.68(2)
Mo1–P2	2.581(1)	Co1–Mo1–Mo2	84.73(2)
Mo2–P2	2.536(1)	C1–Mo1–Mo2	114.5(1)
Co1–P2	2.355(1)	C1–Mo1–P1	121.1(1)
Co2–P2	2.363(1)	C1–Mo1–P2	67.5(1)
Mo1–P3	2.456(1)	C1–Mo1–P3	91.2(1)
Mo2–P3	2.430(1)	C2–Mo2–P1	73.7(1)
Mo1–C1	1.961(4)	C2–Mo2–P2	130.6(1)
Mo2–C2	1.969(4)	C2–Mo2–P3	93.9(1)
P1–C8	1.838(4)	C8–P1–Mo1	122.6(1)
Co1–C4	1.810(4)	C4–Co1–C5	104.1(2)
Co1–C3	1.920(4)	C4–Co1–C3	98.5(2)

phosphinidene clusters of type [Co<sub>4</sub>(μ-CO)<sub>2</sub>(CO)<sub>8</sub>(μ-PR)<sub>2</sub>].<sup>36</sup> The phosphide-metal distances are some 0.13 Å longer than those measured for the corresponding phosphinidene-metal bonds, which is consistent with the relative electron-donor properties of these ligands (three vs four electrons), if assuming the presence of a lone electron pair on the pyramidal phosphide atom. This type of coordination of a μ<sub>4</sub>-phosphide ligand is very unusual; actually, we are aware of just one reported complex displaying a pyramidal phosphide ligand capping a square M<sub>4</sub> skeleton, which happens to be a related tetracobalt cluster, [Co<sub>4</sub>(μ<sub>4</sub>-P)<sub>2</sub>(μ-P<sup>t</sup>Bu<sub>2</sub>)<sub>2</sub>(CO)<sub>8</sub>].<sup>37</sup> In the latter complex, the Co–P distances of ca. 2.29 Å are some 0.07 Å shorter than the corresponding lengths of ca. 2.36 Å in 10, perhaps reflecting a *trans*-influence effect of the phosphinidene on the phosphide ligand in the latter cluster.

Spectroscopic data for 10 in solution are consistent with its solid-state structure. Its IR spectrum in dichloromethane solution displays six bands in the C–O stretching region, with that at the lowest frequency of 1821 cm<sup>−1</sup> being assigned



to the bridging carbonyl. The  $^1\text{H}$  and  $^{13}\text{C}\{^1\text{H}\}$  NMR spectra are in agreement with the absence of any symmetry elements in **10**: thus, two different  $^1\text{H}$  and  $^{13}\text{C}$  resonances are observed for the Cp ligands, and seven distinct resonances are observed for the CO ligands, with that at 291.0 ppm revealing the persistence of a bridging carbonyl in solution. Its  $^{31}\text{P}\{^1\text{H}\}$  NMR spectrum exhibits three distinct resonances in the range of 178–208 ppm, which could be unambiguously assigned through a  $^1\text{H}$ -coupled  $^{31}\text{P}$  spectrum, but their mutual coupling was not as anticipated. In particular, since the phosphinidene P atom is positioned *trans* to the  $\text{PCy}_2$  bridge (average angle of  $102^\circ$  for two P–Mo–P paths) but *cis* to the phosphide ligand (average  $67^\circ$  for four P–M–P paths) we would have expected the PMe/P coupling to be much larger than the PMe/ $\text{PCy}_2$  coupling, which is not consistent with the experimental values of just 9 Hz for both couplings. We trust these anomalous values to be derived from the presence of the lone electron pair at the pyramidal phosphide ligand of **10**, although we have no data on related complexes to be used for comparative purposes. We note, however, that  $^2J_{\text{PP}}$  values in polyphosphorus(III) compounds are quite sensitive to relative orientations of lone electron pairs.<sup>18</sup>

## CONCLUSIONS

The methylidiphosphenyl complex **1** easily incorporates two 16- and/or 14-electron metal carbonyl fragments ( $\text{ML}_n$ ) to give novel tetranuclear complexes displaying a great variety of structures, most of them following from a mild P–P bond cleavage in the diphosphenyl ligand that yields phosphide and phosphinidene ligands bridging the metal centers in different  $\mu_3$ - and  $\mu_4$ -coordination modes. In a few cases ( $\text{ML}_n = \text{MnCp}'(\text{CO})_2$  and  $\text{W}(\text{CO})_5$ ), the metal fragments can be attached to the P atoms without P–P bond cleavage, to give derivatives  $[\text{M}_2\text{Mo}_2\text{Cp}_2(\mu\text{-PCy}_2)(\mu_4\text{-}\kappa^2\text{:}\kappa^1\text{:}\kappa^1\text{-P}_2\text{Me})(\text{CO})_2\text{L}_{2n}]$  having the diphosphenyl ligand coordinated to four metal atoms in an unprecedented, alkenyl-like fashion, but these species were rather unstable. These results are in contrast with those following from incorporation of just one 16-electron fragment, which in many cases involved P–P bond cleavage and release of the PMe ligand. Complex **1** can also add pairs of odd-electron metal carbonyl fragments  $\text{M}(\text{CO})_n$  ( $\text{M} = \text{Mn}, \text{Re}, \text{Co}$ ) upon reaction with the corresponding dimers  $[\text{M}_2(\text{CO})_{2n}]$  under appropriate conditions, whereby the P–P bond in the diphosphenyl ligand is also cleaved to give novel tetranuclear clusters with either open (66 electrons,  $\text{M} = \text{Mn}, \text{Re}$ ) or square-planar (64 electrons,  $\text{M} = \text{Co}$ ) metal cores which display five- and three-electron donor  $\mu_4$ -P ligands with unusual environments (distorted trigonal pyramidal and square pyramidal, respectively).

## EXPERIMENTAL SECTION

**General Procedures and Starting Materials.** All manipulations and reactions were carried out under a nitrogen (99.995%) atmosphere using standard Schlenk techniques. Solvents were purified according to literature procedures and distilled prior to use.<sup>38</sup> All reagents were obtained from the usual commercial suppliers and used as received, unless otherwise stated, except for compounds  $[\text{MnCp}'(\text{CO})_2(\text{THF})]$ ,<sup>39</sup>  $[\text{M}(\text{CO})_5(\text{THF})]$  ( $\text{M} = \text{Mo}, \text{W}$ ),<sup>40</sup>  $[\text{Mo}_2\text{Cp}_2(\mu\text{-PCy}_2)(\mu\text{-}\kappa^2\text{:}\kappa^2\text{-P}_2\text{Me})(\text{CO})_2]$  (**1**),<sup>4</sup> and  $[\text{Mo}_2\text{WCp}_2(\mu_3\text{-P})(\mu\text{-PCy}_2)(\mu_3\text{-PMe})(\text{CO})_6]$  (**3d**),<sup>1</sup> which were prepared as described previously. Photochemical experiments were performed using jacketed Pyrex Schlenk tubes, cooled by tap water (ca. 288 K). A 400 W mercury lamp placed ca. 1 cm away from the Schlenk tube was used for these experiments. A modified literature procedure was employed

in the preparation of the adduct  $[\text{Mo}(\text{CO})_4(\text{THF})_2]$ ,<sup>41</sup> which was obtained at 288 K at low reaction times; IR monitoring was used to determine the optimum reaction time. Petroleum ether refers to that fraction distilling in the range of 338–343 K. Chromatographic separations were carried out using jacketed columns refrigerated by tap water or by a closed 2-propanol circuit kept at the desired temperature with a cryostat. Commercial aluminum oxide (activity I, 150 mesh) was degassed under vacuum prior to use. The latter was mixed under nitrogen with the appropriate amount of water to reach activity IV. IR stretching frequencies of CO ligands were measured in solution (using  $\text{CaF}_2$  windows), or in Nujol mulls, are referred to as  $\nu(\text{CO})$  and are given in wave numbers ( $\text{cm}^{-1}$ ). Nuclear magnetic resonance (NMR) spectra were routinely recorded at 300.13 ( $^1\text{H}$ ), 121.50 ( $^{31}\text{P}\{^1\text{H}\}$ ), or 75.47 MHz ( $^{13}\text{C}\{^1\text{H}\}$ ) at 298 K in  $\text{CD}_2\text{Cl}_2$  solution unless otherwise stated. Chemical shifts ( $\delta$ ) are given in ppm, relative to internal tetramethylsilane ( $^1\text{H}$ ,  $^{13}\text{C}$ ) or external 85% aqueous  $\text{H}_3\text{PO}_4$  solutions ( $^{31}\text{P}$ ). Coupling constants ( $J$ ) are given in Hertz.

**Preparation of  $[\text{Fe}_2\text{Mo}_2\text{Cp}_2(\mu_4\text{-P})(\mu\text{-PCy}_2)(\mu_3\text{-PMe})(\text{CO})_9]$  (**5**).** Solid  $[\text{Fe}_2(\text{CO})_9]$  (0.055 g, 0.150 mmol) was added to a dichloromethane solution (5 mL) of compound **1** (0.040 g, 0.061 mmol), and the mixture was stirred for 1 h to give a brown-orange solution containing a 9 to 1 mixture of compound **5** and the known complex **3a**. Solvent was then removed under vacuum, and the residue was extracted with dichloromethane/petroleum ether (1/9) and chromatographed through alumina. An orange fraction containing **3a** was first eluted and discarded, followed by a green fraction. Removal of solvents from the latter fraction yielded compound **5** as a brown solid (0.031 g, 51%). The crystals of **5** used in the X-ray analysis were grown through the slow diffusion of a layer of petroleum ether into a concentrated dichloromethane solution of the complex at room temperature. Anal. Calcd for  $\text{C}_{32}\text{H}_{35}\text{Fe}_2\text{Mo}_2\text{O}_9\text{P}_3$ : C, 40.03; H, 3.67. Found: C, 40.33; H, 3.70%.  $\nu(\text{CO})$ (Nujol): 2037 (s), 2013 (s), 1972 (s), 1953 (m), 1944 (s), 1933 (m), 1926 (s), 1909 (vs), 1890 (m).  $^1\text{H}$  NMR:  $\delta$  5.54, 5.32 (2s,  $2 \times 5\text{H}$ , Cp), 2.37 (d,  $J_{\text{PH}} = 9$ , 3H, Me), 2.05–1.20 (m, 22H, Cy).  $^{31}\text{P}\{^1\text{H}\}$  NMR:  $\delta$  272.5 (dd,  $J_{\text{PP}} = 191$ , 10,  $\mu\text{-PMe}$ ), 233.4 (dd,  $J_{\text{PP}} = 191$ , 53,  $\mu\text{-P}$ ), 129.8 (dd,  $J_{\text{PP}} = 53$ , 10,  $\mu\text{-PCy}_2$ ).  $^{31}\text{P}$  NMR:  $\delta$  272.5 (dq,  $J_{\text{PP}} = 191$ ,  $J_{\text{PP}} \approx J_{\text{PH}} = 10$ ,  $\mu\text{-PMe}$ ), 233.4 (dd,  $J_{\text{PP}} = 191$ , 53,  $\mu\text{-P}$ ), 129.8 (dm,  $J_{\text{PP}} = 53$ ,  $\mu\text{-PCy}_2$ ).  $^{13}\text{C}\{^1\text{H}\}$  NMR:  $\delta$  235.9 (m, MoCO), 226.2 (d,  $J_{\text{CP}} = 36$ , MoCO), 215.6 [d,  $J_{\text{CP}} = 12$ ,  $\text{Fe}(\text{CO})_3$ ], 91.2, 89.8 (2s, Cp), 39.3 [d,  $J_{\text{CP}} = 8$ ,  $\text{C}^1(\text{Cy})$ ], 38.6 [s,  $\text{C}^2(\text{Cy})$ ], 36.7, 35.7 [2d,  $J_{\text{CP}} = 5$ ,  $\text{C}^2(\text{Cy})$ ], 34.9 [s,  $\text{C}^2(\text{Cy})$ ], 29.6 [d,  $J_{\text{CP}} = 11$ ,  $\text{C}^3(\text{Cy})$ ], 28.8 [d,  $J_{\text{CP}} = 8$ ,  $\text{C}^3(\text{Cy})$ ], 28.4, 27.4 [2d,  $J_{\text{CP}} = 11$ ,  $\text{C}^3(\text{Cy})$ ], 26.6, 26.5 [2s,  $\text{C}^4(\text{Cy})$ ], 26.2 (d,  $J_{\text{CP}} = 9$ , Me).  $^{13}\text{C}\{^1\text{H}\}$  NMR (100.61 MHz, 220 K):  $\delta$  235.4 (m, MoCO), 225.5 (d, br,  $J_{\text{CP}} = 31$ , MoCO), 216.4 [d,  $J_{\text{CP}} = 13$ ,  $\text{FeCO}(\text{ax})$ ], 215.1 [d,  $J_{\text{CP}} = 11$ ,  $\text{Fe}(\text{CO})_3$ ], 209.4 [s, br,  $\text{FeCO}(\text{eq})$ ], 91.0, 89.9 (2s, Cp), 54.7 [d,  $J_{\text{CP}} = 8$ ,  $\text{C}^1(\text{Cy})$ ], 38.02, 38.07 [2s,  $\text{C}^{1,2}(\text{Cy})$ ], 36.4, 35.2 [2d,  $J_{\text{CP}} = 5$ ,  $\text{C}^2(\text{Cy})$ ], 34.4 [s,  $\text{C}^2(\text{Cy})$ ], 29.4 [d,  $J_{\text{CP}} = 11$ ,  $\text{C}^3(\text{Cy})$ ], 28.5 [d,  $J_{\text{CP}} = 7$ ,  $\text{C}^3(\text{Cy})$ ], 28.2, 27.1 [2d,  $J_{\text{CP}} = 11$ ,  $\text{C}^3(\text{Cy})$ ], 26.5 (s, br, Me), 26.3 [s,  $\text{C}^4(\text{Cy})$ ].

**Preparation of Solutions of  $[\text{Mn}_2\text{Mo}_2\text{Cp}_2\text{Cp}'_2(\mu\text{-PCy}_2)(\mu\text{-}\kappa^2\text{:}\kappa^1\text{:}\kappa^1\text{-P}_2\text{Me})(\text{CO})_6]$  (**6b**).** A tetrahydrofuran (THF) solution (5 mL) of the adduct  $[\text{MnCp}'(\text{CO})_2(\text{THF})]$ , prepared *in situ* from  $[\text{MnCp}'(\text{CO})_3]$  (20  $\mu\text{L}$ , 0.125 mmol), was added to a tetrahydrofuran solution (5 mL) of compound **1** (0.020 g, 0.031 mmol), and the mixture was stirred at room temperature for 90 min to give a brown-orange solution containing compound **6b** and the known trinuclear complexes **2b** and **4b** in a ratio of ca. 3:1:3. These compounds decompose upon manipulation to leave **4b** as the only carbonyl-containing product. Spectroscopic data for **6b**:  $^{31}\text{P}\{^1\text{H}\}$  NMR (THF, 162.14 MHz):  $\delta$  143.9 (d, br,  $J_{\text{PP}} \approx 500$ , PMe), 121.1 (s,  $\mu\text{-PCy}_2$ ), –5.4 (d, br,  $J_{\text{PP}} \approx 500$ , PPMe).

**Preparation of Compounds  $[\text{Mo}_2\text{W}_2\text{Cp}_2(\mu\text{-PCy}_2)(\mu\text{-}\kappa^2\text{:}\kappa^1\text{:}\kappa^1\text{-P}_2\text{Me})(\text{CO})_{12}]$  (**6d**) and  $[\text{Mo}_2\text{W}_2\text{Cp}_2(\mu_3\text{-P})(\mu\text{-PCy}_2)(\mu_3\text{-PMe})(\text{CO})_{10}]$  (**7**).** A tetrahydrofuran solution (7 mL) of the adduct  $[\text{W}(\text{CO})_5(\text{THF})]$ , prepared *in situ* from  $[\text{W}(\text{CO})_6]$  (0.055 g, 0.156 mmol), was added to a tetrahydrofuran solution (7 mL) of compound **1** (0.040 g, 0.061 mmol), and the mixture was stirred at room temperature for 40 min. After removal of solvent under vacuum the solid residue was dissolved in toluene (5 mL) and further stirred for 3 h. Then, the solvent was again removed, a tetrahydrofuran solution (7

mL) of  $[\text{W}(\text{CO})_5(\text{THF})]$  (0.060 mmol) was added, and the mixture was stirred for 30 min in this solvent and for 1 h in toluene as described above, to give a brown-orange solution containing a small amount of the known trinuclear complex **4d** along with complexes **6d** and **7** in a 3:2 ratio. After removal of solvent, the residue was extracted with dichloromethane/petroleum ether (1/3) and chromatographed through alumina at 253 K. Elution with dichloromethane/petroleum ether (1/6) gave a red fraction followed by a brown fraction yielding, upon removal of solvents, compounds **7** (red-orange solid, 0.035 g, 35%) and **6d** (orange solid, 0.023 g, 30%), respectively. The crystals of **6d** used in the X-ray analysis were grown through the slow diffusion of layers of diethyl ether and petroleum ether into a concentrated dichloromethane solution of the complex at 253 K. The crystals of **7** were grown through the slow diffusion of a layer of petroleum ether into a concentrated toluene solution of the complex at 253 K. *Spectroscopic data for 6d*: Anal. Calcd for  $\text{C}_{35}\text{H}_{35}\text{Mo}_2\text{O}_{12}\text{P}_3\text{W}_2$ : C, 32.33; H, 2.71. Found: C, 32.65; H, 2.74%.  $^1\text{H NMR}$ :  $\delta$  5.47, 5.34 (2s,  $2 \times 5\text{H}$ , Cp), 2.08 (dd,  $J_{\text{PH}} = 9$ , 4, 3H, Me), 2.60–1.00 (m, 22H, Cy).  $^{31}\text{P}\{^1\text{H}\}$  NMR:  $\delta$  153.4 (d,  $J_{\text{PP}} = 9$ ,  $\mu\text{-PCy}_2$ ), 93.9 (dd,  $J_{\text{PP}} = 431$ ,  $J_{\text{PW}} = 193$ , PMe), –116.5 (d,  $J_{\text{PP}} = 431$ ,  $J_{\text{PW}} = 238$ , PPMe). *Spectroscopic data for 7*: Anal. Calcd for  $\text{C}_{33}\text{H}_{35}\text{Mo}_2\text{O}_{10}\text{P}_3\text{W}_2$ : C, 31.86; H, 2.84. Found: C, 32.24; H, 2.85%.  $^1\text{H NMR}$ :  $\delta$  6.02 (s, 10H, Cp), 2.87, 2.09 (2m,  $2 \times 1\text{H}$ , Cy), 1.82 (d,  $J_{\text{PH}} = 8$ , 3H, Me), 1.90–0.60 (m, 18H, Cy).  $^1\text{H NMR}$  (400.13 MHz, 223 K):  $\delta$  6.04 (s, 10H, Cp), 2.85, 2.10 (2m,  $2 \times 1\text{H}$ , Cy), 1.85 (s, 3H, Me), 1.82–1.72 (m, 4H, Cy), 1.62 (m, 2H, Cy), 1.55–1.10 (m, 9H, Cy), 0.90 (m, 2H, Cy), 0.72 (m, 1H, Cy), –0.10 (m, 2H, Cy).  $^{31}\text{P}\{^1\text{H}\}$  NMR:  $\delta$  941.8 (dd,  $J_{\text{PP}} = 24$ , 19,  $J_{\text{PW}} = 166$ ,  $\mu\text{-P}$ ), 340.6 (dd,  $J_{\text{PP}} = 19$ , 12,  $J_{\text{PW}} = 190$ ,  $\mu\text{-PMe}$ ), 293.2 (dd,  $J_{\text{PP}} = 24$ , 12,  $\mu\text{-PCy}_2$ ).  $^{13}\text{C}\{^1\text{H}\}$  NMR (100.61 MHz, 223 K):  $\delta$  206.4 [d,  $J_{\text{CP}} = 17$ , WCO(ax)], 205.1 [d,  $J_{\text{CP}} = 16$ , WCO(ax)], 200.3 [d,  $J_{\text{CP}} = 3$ , WCO(eq)], 197.1 [d,  $J_{\text{CP}} = 4$ , WCO(eq)], 92.6 (s, Cp), 56.0 (d,  $J_{\text{CP}} = 5$ , Me), 53.6 [d,  $J_{\text{CP}} = 16$ ,  $\text{C}^1(\text{Cy})$ ], 38.0 [d,  $J_{\text{CP}} = 15$ ,  $\text{C}^1(\text{Cy})$ ], 30.9 [s,  $\text{C}^2(\text{Cy})$ ], 29.2 [d,  $J_{\text{CP}} = 2$ ,  $\text{C}^2(\text{Cy})$ ], 26.8 [d,  $J_{\text{CP}} = 10$ ,  $\text{C}^3(\text{Cy})$ ], 26.2 [d,  $J_{\text{CP}} = 11$ ,  $\text{C}^3(\text{Cy})$ ], 25.9, 25.4 [2s,  $\text{C}^4(\text{Cy})$ ].

**Preparation of  $[\text{Mo}_2\text{Cp}_2(\mu_4\text{-P})(\mu\text{-PCy}_2)(\mu_3\text{-PMe})(\text{CO})_9]$  (**8c**).** A tetrahydrofuran solution (5 mL) of the adduct  $[\text{Mo}(\text{CO})_4(\text{THF})_2]$ , prepared *in situ* from  $[\text{Mo}(\text{CO})_6]$  (0.018 g, 0.068 mmol), was added to a tetrahydrofuran solution (5 mL) of compound **1** (0.020 g, 0.030 mmol), and the mixture was stirred at room temperature for 2 h to give a mixture of two unidentified products, along with compound **8c** and the known trinuclear complex **4c**. The solvent was removed under vacuum, and the residue was extracted with dichloromethane/petroleum ether (1/4) and chromatographed through alumina at 253 K. Elution with the same solvent mixture gave first a yellow fraction containing **4c**, which was discarded, and then a green fraction. Removal of solvents from the latter fraction yielded compound **8c** as a green solid (0.018 g, 58%). Anal. Calcd for  $\text{C}_{32}\text{H}_{35}\text{Mo}_2\text{O}_9\text{P}_3$ : C, 36.95; H, 3.39. Found: C, 37.32; H, 3.47%.  $^1\text{H NMR}$ :  $\delta$  5.25 (s, br, 10H, Cp), 2.61 (d,  $J_{\text{PH}} = 13$ , 3H, Me), 2.35–0.90 (m, 22H, Cy).  $^{31}\text{P}\{^1\text{H}\}$  NMR:  $\delta$  663.7 (s, br,  $\mu\text{-P}$ ), 397.9 (dd,  $J_{\text{PP}} = 26$ , 7,  $\mu\text{-PMe}$ ), 178.3 (dd,  $J_{\text{PP}} = 26$ , 7,  $\mu\text{-PCy}_2$ ).  $^{31}\text{P}$  NMR:  $\delta$  663.7 (s, br,  $\mu\text{-P}$ ), 398.0 (m,  $\mu\text{-PMe}$ ), 178.3 (m,  $\mu\text{-PCy}_2$ ).

**Preparation of  $[\text{Mo}_2\text{W}_2\text{Cp}_2(\mu_4\text{-P})(\mu\text{-PCy}_2)(\mu_3\text{-PMe})(\text{CO})_9]$  (**8d**).** A tetrahydrofuran solution (5 mL) of the adduct  $[\text{W}(\text{CO})_5(\text{THF})]$ , prepared *in situ* from  $[\text{W}(\text{CO})_6]$  (0.015 g, 0.043 mmol), was added to a tetrahydrofuran solution (5 mL) of compound **3d** (0.028 g, 0.030 mmol), and the mixture was stirred at room temperature for 30 min. Solvent was then removed under vacuum, and the residue was dissolved in toluene (7 mL) and further stirred for 30 min. This mixture was reacted again with  $[\text{W}(\text{CO})_5(\text{THF})]$  (ca. 0.030 mmol), first in tetrahydrofuran solution (5 mL) for 30 min and then in toluene (5 mL) for a further 30 min. After removal of solvent, the residue was extracted with dichloromethane/petroleum ether (1/4) and chromatographed through alumina at 253 K. Elution with dichloromethane/petroleum ether (1/7) gave first a yellow fraction, which was discarded, and then a brown-greenish fraction. Removal of solvents from the latter fraction yielded compound **8d** as a brown-greenish solid (0.016 g, 43%). Anal. Calcd for  $\text{C}_{32}\text{H}_{35}\text{Mo}_2\text{W}_2\text{O}_9\text{P}_3$ : C, 31.61; H, 2.90.

Found: C, 31.55; H, 2.96%.  $^1\text{H NMR}$ :  $\delta$  5.29 (s, br, 10H, Cp), 2.66 (d,  $J_{\text{PH}} = 13$ , 3H, Me), 2.34–0.95 (m, 22H, Cy).  $^{31}\text{P}\{^1\text{H}\}$  NMR:  $\delta$  554.6 (s, br,  $J_{\text{PW}} = 253$ , 187,  $\mu\text{-P}$ ), 363.7 (dd,  $J_{\text{PP}} = 32$ , 3,  $\mu\text{-PMe}$ ), 167.0 (dd,  $J_{\text{PP}} = 32$ , 7,  $\mu\text{-PCy}_2$ ).  $^{31}\text{P}$  NMR:  $\delta$  554.6 (s, br,  $J_{\text{PW}} = 253$ , 187,  $\mu\text{-P}$ ), 363.7 (dq,  $J_{\text{PP}} = 32$ , 3,  $J_{\text{PH}} = 13$ ,  $\mu\text{-PMe}$ ), 167.0 (m, br,  $\mu\text{-PCy}_2$ ).  $^{13}\text{C}\{^1\text{H}\}$  NMR (100.61 MHz):  $\delta$  213.2 [s, br,  $\text{W}(\text{CO})_4$ ], 200.1 [d,  $J_{\text{CP}} = 6$ , WCO(eq)], 90.6 (s, Cp), 47.0 [d,  $J_{\text{CP}} = 21$ ,  $\text{C}^1(\text{Cy})$ ], 46.0 [d,  $J_{\text{CP}} = 19$ ,  $\text{C}^1(\text{Cy})$ ], 34.7, 34.2 [2s,  $\text{C}^2(\text{Cy})$ ], 28.3, 27.9 [2d,  $J_{\text{CP}} = 12$ ,  $\text{C}^3(\text{Cy})$ ], 26.5 [s,  $\text{C}^4(\text{Cy})$ ], 18.8 (s, Me).  $^{13}\text{C}\{^1\text{H}\}$  NMR (100.61 MHz, 223 K):  $\delta$  212.7 [s, br,  $\text{W}(\text{CO})_4$ ], 200.1 [d,  $J_{\text{CP}} = 6$ , WCO(eq)], 90.5 (s, Cp), 46.0 [d,  $J_{\text{CP}} = 19$ ,  $\text{C}^1(\text{Cy})$ ], 45.4 [d,  $J_{\text{CP}} = 20$ ,  $\text{C}^1(\text{Cy})$ ], 34.4, 34.0 [2s,  $\text{C}^2(\text{Cy})$ ], 27.8 [d,  $J_{\text{CP}} = 12$ ,  $2\text{C}^3(\text{Cy})$ ], 26.4, 26.3 [2s,  $\text{C}^4(\text{Cy})$ ], 19.3 (s, Me); the resonance for the axial carbonyl of the  $\text{W}(\text{CO})_5$  fragment could not be identified in this spectrum.

**Preparation of  $[\text{Mn}_2\text{Mo}_2\text{Cp}_2(\mu_4\text{-P})(\mu\text{-PCy}_2)(\mu_3\text{-PMe})(\text{CO})_9]$  (**9e**).** Solid  $[\text{Mn}_2(\text{CO})_{10}]$  (0.012 g, 0.030 mmol) was added to a toluene solution (6 mL) of **1** (0.020 g, 0.030 mmol), and the mixture was irradiated with visible–UV light for 15 min at 288 K to yield a brown solution. After removal of solvent under vacuum, the residue was extracted with dichloromethane/petroleum ether (1/5) and chromatographed through alumina at 253 K. Elution with the same solvent mixture gave first a yellow fraction, which was discarded, and then a dark green fraction. Removal of solvents from the latter fraction gave compound **9e** as a dark green solid (0.018 g, 63%). The crystals of **9e** used in the X-ray analysis were grown through the slow diffusion of layers of diethyl ether and petroleum ether into a concentrated dichloromethane solution of the complex at 253 K. Anal. Calcd for  $\text{C}_{32}\text{H}_{35}\text{Mn}_2\text{Mo}_2\text{O}_9\text{P}_3$ : C, 40.11; H, 3.68. Found: C, 39.76; H, 3.61%.  $\nu(\text{CO})$ (Nujol): 2047 (vs), 1991 (s), 1962 (s), 1951 (s), 1934 (s), 1901 (s), 1889 (m), 1874 (s).  $^1\text{H NMR}$ :  $\delta$  5.49, 5.23 (2s,  $2 \times 5\text{H}$ , Cp), 2.31 (d,  $J_{\text{PH}} = 7$ , 3H, Me), 2.00–1.05 (m, 22H, Cy).  $^{31}\text{P}\{^1\text{H}\}$  NMR:  $\delta$  419.6 (dd, br,  $J_{\text{PP}} = 306$ , 85,  $\mu\text{-P}$ ), 133.7 (dd,  $J_{\text{PP}} = 306$ , 18,  $\mu\text{-PMe}$ ), 125.3 (dd,  $J_{\text{PP}} = 85$ , 18,  $\mu\text{-PCy}_2$ ).  $^{31}\text{P}$  NMR:  $\delta$  419.2 (dd, br,  $J_{\text{PP}} = 305$ , 85,  $\mu\text{-P}$ ), 133.6 (d, br,  $J_{\text{PP}} = 305$ ,  $\mu_3\text{-PMe}$ ), 125.2 (d, br,  $J_{\text{PP}} = 85$ ,  $\mu\text{-PCy}_2$ ).

**Preparation of  $[\text{Mo}_2\text{Re}_2\text{Cp}_2(\mu_4\text{-P})(\mu\text{-PCy}_2)(\mu_3\text{-PMe})(\text{CO})_9]$  (**9f**).** Solid  $[\text{Re}_2(\text{CO})_{10}]$  (0.025 g, 0.038 mmol) was added to a toluene solution (6 mL) of **1** (0.020 g, 0.030 mmol), and the mixture was irradiated with visible–UV light for 15 min at 288 K to give a brown solution. After removal of solvent, the residue was extracted with dichloromethane/petroleum ether (1/6) and chromatographed through alumina at 253 K. Elution with dichloromethane/petroleum ether (1/10) yielded minor green and blue fractions, which were discarded, and then an orange fraction giving, upon removal of solvents, compound **9f** as an orange solid (0.014 g, 39%). The crystals of **9f** used in the X-ray analysis were grown through the slow diffusion of a layer of petroleum ether into a concentrated dichloromethane solution of the complex at 253 K. Anal. Calcd for  $\text{C}_{32}\text{H}_{35}\text{Mo}_2\text{O}_9\text{P}_3\text{Re}_2$ : C, 31.48; H, 2.89. Found: C, 31.41; H, 2.94%.  $\nu(\text{CO})$ (Nujol): 2069 (vs), 1992 (s), 1980 (vs), 1962 (s), 1934 (s), 1903 (s), 1892 (m), 1876 (s).  $^1\text{H NMR}$ :  $\delta$  5.46, 5.29 (2s,  $2 \times 5\text{H}$ , Cp), 2.22 (d,  $J_{\text{PH}} = 7$ , 3H, Me), 2.10–1.10 (m, 22H, Cy).  $^{31}\text{P}\{^1\text{H}\}$  NMR:  $\delta$  208.7 (dd,  $J_{\text{PP}} = 229$ , 91,  $\mu\text{-P}$ ), 120.4 (dd,  $J_{\text{PP}} = 91$ , 12,  $\mu\text{-PCy}_2$ ), 18.9 (dd,  $J_{\text{PP}} = 229$ , 12,  $\mu\text{-PMe}$ ).  $^{31}\text{P}$  NMR:  $\delta$  208.7 (dd,  $J_{\text{PP}} = 229$ , 91,  $\mu\text{-P}$ ), 120.4 (dm,  $J_{\text{PP}} = 91$ ,  $\mu\text{-PCy}_2$ ), 18.9 (dm,  $J_{\text{PP}} = 229$ ,  $\mu\text{-PMe}$ ).

**Preparation of  $[\text{Co}_2\text{Mo}_2\text{Cp}_2(\mu_4\text{-P})(\mu\text{-PCy}_2)(\mu_4\text{-PMe})(\mu\text{-CO})(\text{CO})_6]$  (**10**).** Solid  $[\text{Co}_2(\text{CO})_8]$  (0.011 g, 0.032 mmol) was added to a toluene solution (6 mL) of compound **1** (0.020 g, 0.030 mmol), and the mixture was stirred for 50 min to give a dark brown solution. Solvent was then removed under vacuum, and the residue was extracted with toluene and filtered through diatomaceous earth. Removal of solvent from the filtrate gave compound **10** as a brown solid (0.027 g, 85%). The crystals of **10** used in the X-ray analysis were grown through the slow diffusion of a layer of petroleum ether into a concentrated toluene solution of the complex at 253 K. Anal. Calcd for  $\text{C}_{30}\text{H}_{35}\text{Co}_2\text{Mo}_2\text{O}_7\text{P}_3$ : C, 39.59; H, 3.88. Found: C, 39.65; H, 3.81%.  $\nu(\text{CO})$ (Nujol): 2019 (s), 2013 (s), 1993 (s), 1985 (s), 1959 (vs), 1950 (s), 1937 (s), 1907 (vs), 1867 (vs), 1831 (s), 1821 (w, sh).  $^1\text{H NMR}$ :  $\delta$  5.47, 5.15 (2s,  $2 \times 5\text{H}$ , Cp), 2.96 (d,  $J_{\text{PH}} = 7$ , 3H, Me), 2.42–1.20 (m, 22H, Cy).  $^{31}\text{P}\{^1\text{H}\}$  NMR:  $\delta$  208.1 (dd,  $J_{\text{PP}} = 42$ , 9,  $\mu\text{-PMe}$ ),

Table 7. Crystal Data for New Compounds

	5	6d	7·1/2C <sub>7</sub> H <sub>8</sub>	9e	9f	10
mol formula	C <sub>32</sub> H <sub>33</sub> Fe <sub>2</sub> Mo <sub>2</sub> O <sub>9</sub> P <sub>3</sub>	C <sub>35</sub> H <sub>35</sub> Mo <sub>2</sub> O <sub>12</sub> P <sub>3</sub> W <sub>2</sub>	C <sub>73</sub> H <sub>78</sub> Mo <sub>4</sub> O <sub>20</sub> P <sub>3</sub> W <sub>4</sub>	C <sub>32</sub> H <sub>35</sub> Mn <sub>2</sub> Mo <sub>2</sub> O <sub>9</sub> P <sub>3</sub>	C <sub>32</sub> H <sub>35</sub> Mo <sub>2</sub> O <sub>9</sub> P <sub>3</sub> Re <sub>2</sub>	C <sub>30</sub> H <sub>35</sub> Co <sub>2</sub> Mo <sub>2</sub> O <sub>7</sub> P <sub>3</sub>
mol wt	960.09	1300.12	2580.30	958.27	1220.81	910.23
cryst syst	triclinic	monoclinic	monoclinic	monoclinic	monoclinic	monoclinic
space group	$\bar{P}1$	$P2_1$	$P2_1/c$	$P2_1/c$	$P2_1/c$	$P2_1/c$
radiation ( $\lambda$ , Å)	0.710 73	1.541 84	0.710 73	0.710 73	0.710 73	1.541 84
a, Å	10.575(5)	9.7933(4)	19.956(3)	14.6509(10)	14.6140(7)	11.7503(3)
b, Å	11.884(5)	16.7512(5)	10.6471(11)	15.6537(10)	15.6639(8)	17.2964(4)
c, Å	15.513(5)	12.9168(4)	21.872(3)	21.1404(12)	21.4374(9)	18.4643(5)
$\alpha$ , deg	74.117(5)	90	90	90	90	90
$\beta$ , deg	74.843(5)	107.248(3)	117.684(10)	133.254(3)	132.801(3)	118.712(2)
$\gamma$ , deg	73.097(5)	90	90	90	90	90
V, Å <sup>3</sup>	1758.7(13)	2023.70(12)	4115.3(9)	3531.2(4)	3600.6(3)	3291.24(14)
Z	2	2	2	4	4	4
calcd density, g cm <sup>-3</sup>	1.813	2.134	2.082	1.803	2.252	1.837
absorp coeff, mm <sup>-1</sup>	1.694	16.826	6.337	1.580	7.567	15.616
temperature, K	100.0(1)	123.0(1)	100.0(1)	100.0(1)	100.0(1)	123.0(1)
$\theta$ range (deg)	1.39 to 26.02	4.45 to 69.36	1.87 to 26.37	1.86 to 26.37	1.83 to 26.37	3.74 to 69.35
index ranges (h, k, l)	-12, 13; -13, 14; 0, 19	-11, 9; -20, 14; -15, 13	-24, 22; -13, 0; -27, 21	-18, 18; -19, 0; -17, 26	-18, 18; -19, 0; -26, 17	-14, 12; -20, 18; -21, 22
no. of refls collected	26 682	7781	179 760	55 042	82 586	12 507
no. of indep refls (R <sub>int</sub> )	6889 (0.0547)	5270 (0.0501)	8414 (0.0389)	7235 (0.0769)	7371 (0.0461)	5963 (0.0388)
reflens with I > 2 $\sigma$ (I)	5481	5009	7879	5434	6450	5317
R indexes [data with I > 2 $\sigma$ (I)] <sup>a</sup>	R <sub>1</sub> = 0.0412 wR <sub>2</sub> = 0.0604 <sup>b</sup>	R <sub>1</sub> = 0.0529 wR <sub>2</sub> = 0.1399 <sup>c</sup>	R <sub>1</sub> = 0.0147 wR <sub>2</sub> = 0.0304 <sup>d</sup>	R <sub>1</sub> = 0.0360 wR <sub>2</sub> = 0.0580 <sup>e</sup>	R <sub>1</sub> = 0.0215 wR <sub>2</sub> = 0.0396 <sup>f</sup>	R <sub>1</sub> = 0.0342 wR <sub>2</sub> = 0.0860 <sup>g</sup>
R indexes (all data) <sup>a</sup>	R <sub>1</sub> = 0.0587 wR <sub>2</sub> = 0.0670 <sup>b</sup>	R <sub>1</sub> = 0.0560 wR <sub>2</sub> = 0.1441 <sup>c</sup>	R <sub>1</sub> = 0.0170 wR <sub>2</sub> = 0.0310 <sup>d</sup>	R <sub>1</sub> = 0.0639 wR <sub>2</sub> = 0.0650 <sup>e</sup>	R <sub>1</sub> = 0.0293 wR <sub>2</sub> = 0.0416 <sup>f</sup>	R <sub>1</sub> = 0.0400 wR <sub>2</sub> = 0.0910 <sup>g</sup>
GOF	1.069	1.051	1.037	1.013	1.032	1.024
no. of restraints/params	0/419	81/488	0/511	0/434	0/434	0/398
$\Delta\rho$ (max, min), e·Å <sup>-3</sup>	0.841, -0.708	1.947, -1.508	1.569, -0.582	1.223, -0.740	1.660, -1.294	0.986, -0.972

<sup>a</sup>R =  $\sum ||F_0| - |F_c|| / \sum F_0$ . <sup>b</sup>wR =  $[\sum w(|F_0|^2 - |F_c|^2)^2 / \sum w|F_0|^2]^{1/2}$ . <sup>c</sup>w =  $1/[\sigma^2(F_0^2) + (aP)^2 + bP]$ , where  $P = (F_0^2 + 2F_c^2)/3$ . <sup>d</sup>a = 0.0141, b = 1.3342. <sup>e</sup>a = 0.0916, b = 12.1091. <sup>f</sup>a = 0.0108, b = 6.2593. <sup>g</sup>a = 0.0146, b = 6.4099. <sup>h</sup>a = 0.0129, b = 8.2979. <sup>i</sup>a = 0.0532, b = 0.0830.

184.9 (t, J<sub>PP</sub> = 9,  $\mu$ -PCy<sub>2</sub>), 178.6 (d, br, J<sub>PP</sub> = 42,  $\mu$ -P). <sup>31</sup>P NMR:  $\delta$  208.1 (m, br, J<sub>PP</sub> = 42,  $\mu$ -PMe), 184.9 (s, br,  $\mu$ -PCy<sub>2</sub>), 178.6 (d, br, J<sub>PP</sub> = 42,  $\mu$ -P). <sup>13</sup>C{<sup>1</sup>H} NMR (100.61 MHz, 233 K):  $\delta$  291.0 (s, br,  $\mu$ -CO), 246.8 (s, MoCO), 231.7 (s, br, MoCO), 226.8, 205.8, 204.9, 201.8 (4s, CoCO), 90.2, 85.3 (2s, Cp), 49.7, 47.7 [2s, br, C<sup>1</sup>(Cy)], 35.0 [s, C<sup>2</sup>(Cy)], 33.7 [s, 2C<sup>2</sup>(Cy)], 33.2 [d, br, J<sub>CP</sub> = 5, C<sup>2</sup>(Cy)], 30.2 (d, J<sub>CP</sub> = 13, Me), 28.4, 28.2 [2d, J<sub>CP</sub> = 8, C<sup>3</sup>(Cy)], 28.1 [d, J<sub>CP</sub> = 9, C<sup>3</sup>(Cy)], 27.9 [d, J<sub>CP</sub> = 12, C<sup>3</sup>(Cy)], 26.6, 26.4 [2s, C<sup>4</sup>(Cy)].

**X-ray Structure Determination of Compounds 5, 7, 9e, and 9f.** X-ray intensity data for these compounds were collected on a Kappa-Apex-II Bruker diffractometer using graphite-monochromated Mo K $\alpha$  radiation at 100 K. The software APEX<sup>42</sup> was used for collecting frames with  $\omega/\phi$  scans measurement method. The Bruker SAINT software was used for data reduction,<sup>43</sup> and a multiscan absorption correction was applied with SADABS.<sup>44</sup> Using the program suite WINGX,<sup>45</sup> the structures were generally solved by Patterson interpretation and phase expansion using SHELXL97,<sup>46</sup> except for compound 5, solved by direct methods using Sir92.<sup>47</sup> All structures were refined with full-matrix least-squares on  $F^2$  using SHELXL97. All positional parameters and anisotropic temperature factors for all non-H atoms were refined anisotropically, except for C(8), C(15), and C(18) in 5, and C(42) in 7, which had to be refined isotropically to prevent their temperature factors from becoming nonpositive definite. All hydrogen atoms were geometrically placed and refined using a riding model. Compound 7 was found to crystallize with a molecule of toluene placed on the symmetry element  $-x, 2 - y, 1 - z$  and disordered over two positions, satisfactorily modeled with 0.5 occupancies.

**X-ray Structure Determination of Compounds 6d and 10.** Data collection for these compounds was performed at 123.0(1) K on an Oxford Diffraction Xcalibur Nova single-crystal diffractometer, using Cu K $\alpha$  radiation ( $\lambda$  = 1.5418 Å). Images were collected at a 63 mm fixed crystal-detector distance, using the oscillation method, with

1° oscillation and 1.5 s (6d) or variable exposure time (1.3–5 s for 10) per image. Data collection strategy was calculated with the program *CrysAlis Pro CCD*,<sup>48</sup> and data reduction and cell refinement was performed with the program *CrysAlis Pro RED*.<sup>48</sup> An empirical absorption correction was applied using the SCALE3 ABSPACK algorithm as implemented in the program *CrysAlis Pro RED*. The structures were solved by Patterson interpretation and phase expansion (6d), or by direct methods (10), and were refined with full-matrix least-squares on  $F^2$  using SHELXL97.<sup>46</sup> All positional parameters and temperature factors for non-H atoms were refined anisotropically, except for three atoms in 6d, which had to be refined isotropically in combination with the instructions DELU and SIMU. All hydrogen atoms were geometrically placed and refined using a riding model. Crystallographic data and structure refinement details for all these compounds are collected in Table 7.

## ■ ASSOCIATED CONTENT

### 📄 Supporting Information

A CIF file containing full crystallographic data for compounds 5, 6d, 7, 9e, 9f, and 10 (CCDC 1039075–1039080). This material is available free of charge via the Internet at <http://pubs.acs.org>.

## ■ AUTHOR INFORMATION

### Corresponding Authors

\*E-mail: ara\_12\_79@hotmail.com. (A.R.)

\*E-mail: mara@uniovi.es. (M.A.R.)

### Notes

The authors declare no competing financial interest.



## ACKNOWLEDGMENTS

We thank the DGI of Spain for financial support (Project No. CTQ2012-33187) and the Universidad de Oviedo and Universidad de Santiago de Compostela (X-ray units) for acquisition of diffraction data. A.R. thanks the Spanish Research Council for Scientific Research (CSIC) for a JAE-Doc contract, cofunded by the European Social Fund (ESF).

## REFERENCES

- (1) Alvarez, M. A.; García, M. E.; García-Vivó, D.; Lozano, R.; Ramos, A.; Ruiz, M. A. *Inorg. Chem.* **2014**, *53*, 11261.
- (2) Weber, L.; Schumann, H. *Chem. Ber.* **1991**, *124*, 265.
- (3) Scherer, O. J.; Ehses, M.; Wolmershäuser, G. *Angew. Chem., Int. Ed.* **1998**, *37*, 507.
- (4) (a) Alvarez, M. A.; García, M. E.; García-Vivó, D.; Ramos, A.; Ruiz, M. A. *Inorg. Chem.* **2011**, *50*, 2064. (b) Alvarez, M. A.; García, M. E.; García-Vivó, D.; Ramos, A.; Ruiz, M. A. *Inorg. Chem.* **2012**, *51*, 11061.
- (5) For some reviews on transition metal-mediated activation of  $P_4$ , see: (a) Serrano-Ruiz, M.; Romerosa, A.; Lorenzo-Luis, P. *Eur. J. Inorg. Chem.* **2014**, *10*, 1587. (b) Cossairt, B. M.; Piro, N. A.; Cummins, C. C. *Chem. Rev.* **2010**, *110*, 4164. (c) Caporali, M.; Gonsalvi, L.; Rossini, A.; Peruzzini, M. *Chem. Rev.* **2010**, *110*, 4178. (d) Peruzzini, M.; Gonsalvi, L.; Romerosa, A. *Chem. Soc. Rev.* **2005**, *34*, 1038. (e) Peruzzini, M.; Abdreimova, R. R.; Budnikova, Y.; Romerosa, A.; Scherer, O. J.; Sitzmann, H. *J. Organomet. Chem.* **2004**, *689*, 4319.
- (6) For some reviews on main group element-mediated activation of  $P_4$ , see: (a) Giffin, N. A.; Masuda, J. D. *Coord. Chem. Rev.* **2011**, *255*, 1342. (b) Scheer, M.; Balázs, G.; Seitz, A. *Chem. Rev.* **2010**, *110*, 4236.
- (7) For some recent work on transition metal-mediated activation of  $P_4$ , see: (a) Camp, C.; Maron, L.; Bergman, R. G.; Arnold, J. *J. Am. Chem. Soc.* **2014**, *136*, 17652. (b) Caporali, M.; Gonsalvi, L.; Mirabello, V.; Ienco, A.; Manca, G.; Zanobini, F.; Peruzzini, M. *Eur. J. Inorg. Chem.* **2014**, *10*, 1652. (c) Heinel, S.; Reisinger, S.; Schwarzmaier, C.; Bodensteiner, M.; Scheer, M. *Angew. Chem., Int. Ed.* **2014**, *53*, 7639.
- (8) For some recent work on main group element-mediated activation of  $P_4$ , see: (a) Borger, J. E.; Ehlers, A. W.; Lutz, M.; Slootweg, J. C.; Lammerstma, K. *Angew. Chem., Int. Ed.* **2014**, *53*, 12836. (b) Schoeller, W. W.; Frey, G. D. *Inorg. Chem.* **2014**, *53*, 4840.
- (9) (a) Alvarez, C. M.; Alvarez, M. A.; García, M. E.; García-Vivó, D.; Ruiz, M. A. *Organometallics* **2005**, *24*, 4122. (b) García, M. E.; García-Vivó, D.; Ruiz, M. A. *Organometallics* **2008**, *27*, 543.
- (10) Alvarez, M. A.; García, M. E.; Martínez, M. E.; Menéndez, S.; Ruiz, M. A. *Organometallics* **2010**, *29*, 710.
- (11) Cordero, B.; Gómez, V.; Platero-Prats, A. E.; Revés, M.; Echeverría, J.; Cremades, E.; Barragán, F.; Alvarez, S. *Dalton Trans.* **2008**, 2832.
- (12) Alvarez, C. M.; Alvarez, M. A.; García, M. E.; González, R.; Ramos, A.; Ruiz, M. A. *Inorg. Chem.* **2011**, *50*, 10937 and references therein.
- (13) (a) Collins, B. E.; Koide, Y.; Schauer, C. K.; White, P. S. *Inorg. Chem.* **1997**, *36*, 6172. (b) Koide, Y.; Bautista, M. T.; White, P. S.; Schauer, C. K. *Inorg. Chem.* **1992**, *31*, 3690.
- (14) Bautista, M. T.; White, P. S.; Schauer, C. K. *J. Am. Chem. Soc.* **1991**, *113*, 8963.
- (15) Bautista, M. T.; White, P. S.; Schauer, C. K. *J. Am. Chem. Soc.* **1994**, *116*, 2143.
- (16) Vogel, U.; Sekar, P.; Ahlrichs, R.; Huniar, U.; Scheer, M. *Eur. J. Inorg. Chem.* **2003**, 1518.
- (17) Braterman, P. S. *Metal Carbonyl Spectra*; Academic Press: London, U.K., 1975.
- (18) Jameson, C. J. In *Phosphorus-31 NMR Spectroscopy in Stereochemical Analysis*; Verkade, J. G., Quin, L. D., Eds.; VCH: Deerfield Beach, FL, 1987; Chapter 6.
- (19) A general trend established for  $^2J_{XY}$  in complexes of the type  $[MCpXYL_2]$  is that  $|J_{cis}| > |J_{trans}|$ . See, for instance, reference 18 and also Wrackmeyer, B.; Alt, H. G.; Maisel, H. E. *J. Organomet. Chem.* **1990**, *399*, 125.
- (20) Attali, S.; Dahan, F.; Mathieu, R.; Caminade, A. M.; Majoral, J. P. *J. Am. Chem. Soc.* **1988**, *110*, 1990.
- (21) Aroney, M. J.; Buys, I. E.; Davies, M. S.; Hambley, T. W. *J. Chem. Soc., Dalton Trans.* **1994**, 2827.
- (22) Schollhammer, P.; Pétilion, F. Y.; Poder-Guillou, S.; Talarmin, J.; Muir, K. W.; Yufit, D. S. *J. Organomet. Chem.* **1996**, *513*, 181.
- (23) Alvarez, M. A.; García, M. E.; Ramos, A.; Ruiz, M. A. *J. Organomet. Chem.* **2009**, *694*, 3864.
- (24) Adatia, T.; McPartlin, M.; Mays, M. J.; Morris, M. J.; Raithby, P. R. *J. Chem. Soc., Dalton Trans.* **1989**, 1555.
- (25) Arif, A. M.; Cowley, A. H.; Norman, N. C.; Orpen, A. G.; Pakulski, M. *Organometallics* **1988**, *7*, 309.
- (26) (a) Amor, I.; García, M. E.; Ruiz, M. A.; Sáez, D.; Hamidov, H.; Jeffery, J. C. *Organometallics* **2006**, *25*, 4857. (b) Alvarez, M. A.; Amor, I.; García, M. E.; García-Vivó, D.; Ruiz, M. A.; Sáez, D.; Hamidov, H.; Jeffery, J. C. *Inorg. Chim. Acta* **2015**, *424*, 103.
- (27) García-Vivó, D.; Ramos, A.; Ruiz, M. A. *Coord. Chem. Rev.* **2013**, *257*, 2143.
- (28) García, M. E.; Riera, V.; Ruiz, M. A.; Rueda, M. T.; Sáez, D. *Organometallics* **2002**, *21*, 5515.
- (29) Alvarez, M. A.; García, M. E.; García-Vivó, D.; Martínez, M. E.; Ruiz, M. A. *Organometallics* **2011**, *30*, 2189.
- (30) Scheer, M.; Himmel, D.; Kuntz, C.; Zhan, S.; Leiner, E. *Chem.—Eur. J.* **2008**, *14*, 9020.
- (31) Churchill, M. R.; Amoh, K. N.; Wasserman, H. J. *Inorg. Chem.* **1981**, *20*, 1609.
- (32) Decken, A.; Bottomley, F.; Wilkins, B. E.; Gill, E. D. *Organometallics* **2004**, *23*, 3683.
- (33) Ghosh, S.; Khatun, M.; Haworth, D. T.; Lindeman, S. V.; Siddiquee, T. A.; Bennett, D. W.; Hogarth, G.; Nordlander, E.; Kabir, S. E. *J. Organomet. Chem.* **2009**, *694*, 2941.
- (34) Burck, S.; Götz, K.; Kaupp, M.; Nieger, M.; Weber, J.; Schemedt auf der Günne, J.; Gudat, D. *J. Am. Chem. Soc.* **2009**, *131*, 10763.
- (35) Carty, A. J.; MacLaughlin, S. A.; Nucciarone, D. In *Phosphorus-31 NMR Spectroscopy in Stereochemical Analysis*; Verkade, J. G., Quin, L. D., Eds.; VCH: Deerfield Beach, FL, 1987; Chapter 16.
- (36) (a) Sanchez-Nieves, J.; Sterenberg, B. T.; Udachin, K. A.; Carty, A. J. *Can. J. Chem.* **2004**, *82*, 1507. (b) Fenske, D.; Queisser, J.; Schottmuller, H. Z. *Anorg. Allg. Chem.* **1996**, *622*, 1731. (c) Richmond, M. G.; Kochi, J. K. *Organometallics* **1987**, *6*, 777. (d) Lindner, E.; Weiss, G. A.; Hiller, W.; Fawzi, R. *J. Organomet. Chem.* **1986**, *312*, 365.
- (37) Krautscheid, H.; Matern, E.; Fritz, G.; Pikies, J. Z. *Anorg. Allg. Chem.* **2000**, *626*, 1087.
- (38) Armarego, W. L. F.; Chai, C. *Purification of Laboratory Chemicals*, 5th ed.; Butterworth-Heinemann: Oxford, U.K., 2003.
- (39) Hermann, W. W. *Angew. Chem.* **1974**, *86*, 345.
- (40) Strohmeier, W. *Angew. Chem.* **1964**, *76*, 873.
- (41) Gibson, V. C.; Long, N. J.; Long, R. J.; White, A. J. P.; Williams, C. K.; Williams, D. J.; Grigiotti, E.; Zanello, P. *Organometallics* **2004**, *23*, 957.
- (42) APEX 2, version 2.0–1; Bruker AXS Inc.: Madison, WI, 2005.
- (43) SMART & SAINT Software Reference Manuals, Version 5.051 (Windows NT Version); Bruker Analytical X-ray Instruments: Madison, WI, 1998.
- (44) Sheldrick, G. M. SADABS, Program for Empirical Absorption Correction; University of Göttingen: Göttingen, Germany, 1996.
- (45) Farrugia, L. J. *J. Appl. Crystallogr.* **1999**, *32*, 837.
- (46) Sheldrick, G. M. *Acta Crystallogr.* **2008**, *A64*, 112.
- (47) Altomare, A.; Casciarano, G.; Giacovazzo, C.; Guagliardi, A.; Burla, M. C.; Polidori, G.; Camalli, M. *J. Appl. Crystallogr.* **1994**, *27*, 435.
- (48) CrysAlis Pro; Oxford Diffraction Limited, Ltd.: Oxford, U.K., 2006.